

THE PENNSYLVANIA STATE UNIVERSITY  
SCHREYER HONORS COLLEGE

DEPARTMENT OF MECHANICAL AND NUCLEAR ENGINEERING

DEVELOPING A NEW MODELING METHOD FOR LIQUID PISTON STIRLING  
ENGINES USING THERMAL-HYDRAULIC CODE

ANDREW KRIEBEL  
SPRING 2014

A thesis  
submitted in partial fulfillment  
of the requirements  
for a baccalaureate degree  
in Mechanical Engineering  
with honors in Mechanical Engineering

Reviewed and approved\* by the following:

Andrew M. Erdman  
Walter L. Robb Director of Engineering Leadership Development  
Thesis Supervisor

Dominic Santavicca  
Professor of Mechanical Engineering  
Honors Adviser

\* Signatures are on file in the Schreyer Honors College.

## ABSTRACT

For developing and remote regions of the world, solar powered water pumps provide relief to the usually physical and time intensive task of gathering water. Heat engines are a low-cost alternative to photovoltaic solar cells for providing power for water pumping with concentrated solar energy. Theoretically the most efficient type of heat engine, stirling engines are designed around the stirling cycle [1]. Liquid piston stirling engines are one variant that are particularly useful for water pumping. This variant substitutes oscillating columns of liquid for mechanical pistons. Liquid pistons allow for a tighter piston seal and more efficient designs for heat transfer [8]. In addition, liquid pistons allow the work output of the engine to be directly applied for the pumping of water.

This goal of this paper is to advance the development process of liquid piston stirling engines by validating a new, simpler computer modeling technique. Using the SNAP platform and TRACE thermal-hydraulic computational code developed by the U.S. Nuclear Regulatory Commission, I develop and document a method for modeling and testing liquid piston stirling engines through a graphical interface, finite volume solver with pre and post processing capabilities. This method greatly reduces the time and cost of traditional modeling purposes either through mathematical equations or physical prototyping. Future researchers and developers can use SNAP/TRACE confidently to model and test liquid piston stirling engine designs.

## TABLE OF CONTENTS

Abstract .....	i
Table of Contents .....	ii
Nomenclature .....	iv
Acronyms .....	v
List of Figures .....	vi
List of Tables .....	viii
Acknowledgements .....	ix
Chapter 1 Introduction .....	1
Background and Motivation .....	1
Overview of Kinematic Stirling Engines .....	2
Overview of Liquid Piston Stirling Engines .....	4
Overview of TRACE Thermal-Hydraulic Code .....	5
Research Goals and Approach .....	6
Chapter 2 Review of Relevant Literature .....	7
Liquid Piston Stirling Engine Research .....	8
Designing and Testing Liquid Piston Stirling Engines .....	9
Mathematical Models and Simulations of Liquid Piston Stirling Engines .....	10
Differentiation and Conclusion .....	11
Chapter 3 Designing a Liquid Piston Stirling Engine .....	13
Displacer Design .....	15
Dead Volume .....	16
Tuning-Line Design .....	17
Insulation, Connections, and Heat Transfer .....	18
Summary of Design Decisions .....	19
Ideal Power Output .....	20
Flow and Heat Losses .....	21
Chapter 4 Validation of Modeling Technique Using Discrete Components .....	23
U-Tube Displacer Piston .....	23
U-Tube Displacer with Tuning-line .....	26
Heating and Cooling .....	28
Simple Pump Setup .....	31

Chapter 5 Liquid Piston Stirling Engine Modeled in TRACE .....	34
Displacer U-Tube and Tuning Line .....	34
Dead Volume Components .....	36
Testing the Setup.....	38
Adding the Pumping Arm .....	42
Testing the Final Design .....	44
Chapter 6 Modeling Validated Engine Designs.....	45
West's Laboratory Engine.....	45
Swarthmore Experimental Engine .....	51
Chapter 7 Results, Conclusions, and Recommendations.....	59
Results .....	59
Conclusions .....	61
Recommendations .....	63
Appendix A Model Settings.....	65
Appendix B West Engine Model Geometry .....	71
BIBLIOGRAPHY .....	83

## NOMENCLATURE

$A$	Area, $m^2$
$B_n$	Beale Number
$d, D$	Diameter
$f$	frequency, $1/s$
$g$	Gravitational Constant, $9.81 \text{ m/s}^2$
$h$	Height, $m$
$L$	Length, $m$
$h$	Height, $m$
$\rho$	Density, $kg/m^3$
$P$	Pressure, $Pa$
$s$	Stroke, $m$
$T$	Temperature, $^{\circ}C$ or $K$
$W$	Power, $W$
$V$	Volume, $m^3$
$\dot{V}$	Volume Flow Rate, $m^3/s$

### Subscripts

$h$	Hot
$c$	Cold
$o$	Initial
$disp$	Displacer
$US$	Unswept
$pump$	Pump
$connect$	Connector
$regen$	Regenerator
$heater$	Heater
$tl$	Tunling Line

## ACRONYMS

LPSE	Liquid Piston Stirling Engine
NRC	Nuclear Regulatory Commission
SNAP	Symbolic Nuclear Analysis Package
TRACE	TRAC/RELAP Advanced Computational Engine

## LIST OF FIGURES

Figure 1-1: Action of the displacer piston .....	2
Figure 1-2: Displacer piston drives the power piston .....	3
Figure 1-3: Displacer and power piston action in an LPSE .....	4
Figure 3-1: Sample design configuration with tuning line and pump set-up.....	14
Figure 3-2: LPSE design configuration .....	19
Figure 4-1: SNAP U-Tube design.....	23
Figure 4-2: Gas fraction of right side showing cylinder height .....	25
Figure 4-3: Gas fraction of left side to right side .....	25
Figure 4-4: Mass flow measurements in middle of u-tube .....	25
Figure 4-5: SNAP model for U-Tube with Tuning Line .....	27
Figure 4-6: Oscillations of tuning line, hot side, and cold side .....	28
Figure 4-7: SNAP model with heating components and simple pump output .....	29
Figure 4-8: Temperature fluctuations in the air connection tube.....	30
Figure 4-9: Water level changes in the output tube .....	30
Figure 4-10: Pressure fluctuations in the air connection tube.....	30
Figure 4-11: SNAP pump model .....	31
Figure 4-12: Pressure fluctuations in the tee.....	33
Figure 4-13: Mass flow through bottom and top check valves.....	33
Figure 4-14: Water level changes in pumping arm and output tube.....	33
Figure 5-1: Oscillation occurring in the hot cylinder.....	38
Figure 5-2: Free oscillations in the hot side cylinder with no friction.....	39
Figure 5-3: Oscillation in the tuning line damped by friction .....	40
Figure 5-4: Oscillations in the hot cylinder, cold cylinder , and tuning line .....	40
Figure 5-5: Pressure oscillation in the engine show sustained oscillation with friction .....	40

Figure 5-6: LPSE model before attaching pump arm .....	42
Figure 5-7: LPSE model with pump arm .....	43
Figure 6-1: West's laboratory engine design .....	46
Figure 6-2: TRACE model of West's laboratory engine .....	49
Figure 6-3: Water level oscillation in the hot side cylinder .....	50
Figure 6-4: Pressure oscillations in the air tube connector .....	51
Figure 6-5: Mass flow through the top and bottom check valves .....	51
Figure 6-6: Swarthmore engine schematic with pumping line .....	51
Figure 6-7: Swarthmore engine final design without pumping line .....	52
Figure 6-8: Model of Swarthmore engine final design .....	54
Figure 6-9: Pressure variation measured in Swarthmore engine .....	55
Figure 6-10: Pressure variations in the model .....	55
Figure 6-11: Temperature variations in Swarthmore heat exchanger .....	56
Figure 6-12: Temperature variations in the model heat exchanger .....	56
Figure 6-13: Temperature variations in the Swarthmore hot cylinder .....	57
Figure 6-14: Temperature variations in the model hot cylinder .....	57



**LIST OF TABLES**

Table 2-1: Summary of previous research .....	7
Table 3-1: Possible tuning line configurations .....	18
Table 3-2: Design summary .....	19
Table 6-1: Swarthmore engine design specifications .....	53

## ACKNOWLEDGEMENTS

I would like to express my deepest gratitude to my thesis supervisor, Andrew M. Erdman, whom inspired my research into stirling engines. Since I met him, he has been an excellent advisor and mentor to me. I would also like to thank my thesis and academic advisor, Dominic Santavicca, for his academic guidance and advice on this project. Additionally, I would like to thank Michael Alley, an academic and professional mentor in research and communication. For his help and expertise in TRACE/SNAP, I would like to thank Justin Watson from Penn State ARL.

Many thanks to all of those in State College and Penn State who have made the past four years of my life so enjoyable and meaningful. I owe a great deal of appreciation to my professors, instructors, advisors, and classmates who have inspired my hard work and academic achievements. Additionally, I need to thank my family and friends; without their encouragement and support this would not have been possible. Finally, I would like to thank my parents for their continued support and love throughout my life.

## **Chapter 1**

### **Introduction**

In thermodynamics, a heat engine is any device that operates on a thermodynamic cycle and converts thermal or heat energy into mechanical work. This is possible by extracting energy from a working fluid, bringing it from a higher temperature to a lower temperature [1]. The Stirling engine is a heat engine based around the Stirling cycle. Theoretically, stirling engines have a thermal efficiency equal to that of the Carnot Cycle, the most efficient heat engine cycle possible [8]. For this paper, I will refer to two variations of stirling engines: traditional, kinematic stirling engines with mechanical pistons, and liquid piston stirling engines where the mechanical pistons are replaced with liquid pistons.

### **Background and Motivation**

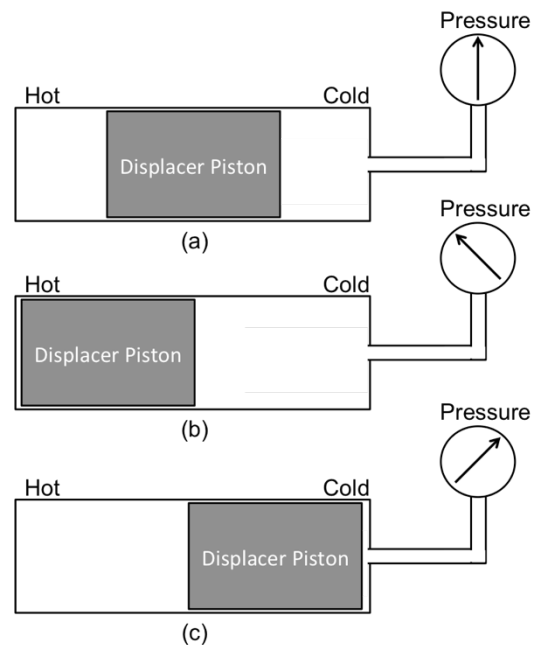
In developing countries and remote regions, where access to modern infrastructure is not possible, accessing water is often a physically intensive and time extensive process. In locations like these, where cost is a major consideration and sunlight is often abundant, there is a need for low-cost, solar-powered pumps to aid in the provision of water. Photovoltaic cells are often used to provide solar-electric power to pumps, but are expensive to install and maintain. Due to their relative simplicity, low-cost, and versatility, stirling engines are one potential alternative for solar-powered water pumping. One stirling engine variant particularly attractive for water pumping is the liquid piston stirling engine (LPSE).

Liquid piston stirling engines have the advantage of using fluidic pistons, which conform to the volume of the piston housings, eliminating the need for mechanical seals. In kinematic stirling engines, the oscillating pressure inside the engine is used to drive a mechanical power

piston. In LPSEs, the oscillating pressure is used as pumping head to pump water out of the engine through a one-way check valve and pull water into the engine through another valve. Since the liquid piston is often water, it has the advantage of being compatible with the fluid being pumped. The purpose of this experimentation is to further the understanding of LPSEs through computer modeling, so that a feasible design may be developed to aid in the provision of water in developing countries and remote regions.

### Overview of Kinematic Stirling Engines

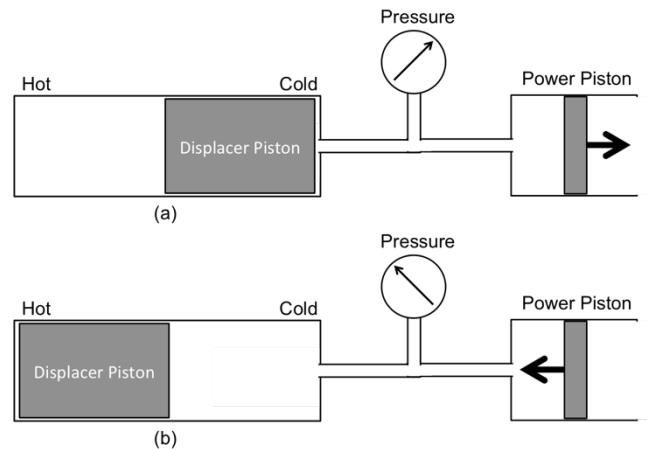
Developed by Robert Stirling in 1816, the stirling engine was developed as an alternative to the steam engine and was used as a water pump in quarries. The engine has two pistons: a displacer piston and a power piston. The displacer piston essentially just takes up space to displace the working fluid to the other side of the engine. The power piston is the power output of the engine that reacts to the pressure changes in the engine. It is easiest to explain the operation of an engine by starting with the displacer piston. Figure 1-1 shows a displacer piston inside of a piston cylinder where one end of the cylinder is hot and the other side is cold. There is a pressure gauge showing the relative pressure inside the cylinder. Since this is a closed system, the volume is constant. In Figure 1-1a the displacer piston is in the middle of the stroke so that the air is equally displaced to both sides of the cylinder and the pressure gauge reads the mean pressure of the system. In Figure 1-1b the displacer piston has



**Figure 1-1: Action of the displacer piston**

moved to the hot side of the engine so that the working fluid is displaced to the cold side of the engine. Because the working fluid is being cooled, the pressure gauge reads lower than before. Alternatively, in 1c the displacer piston is located on the cold side of the engine so that the working fluid has been displaced to the hot side of the engine. Because the working fluid is being heated at constant volume, the pressure gauge reads higher.

To make this process produce work, the oscillating pressure is used to move a power piston. This can be seen in Figure 1-2, in which a power piston has been added and its motion is depicted with arrows. In Figure 1-2a, when the system is at high pressure as it was in Figure 1-1c, the higher pressure drives out the power piston. In Figure 1-2b, when the system is at low pressure as it was in Figure 1-1b, the lower pressure aids in pushing the power piston in. In a kinematic engine, the pistons are connected to each other, typically on a flywheel so that they are 90° out of phase. In other words,



**Figure 1-2: Displacer action drives the power piston**

as seen in Figure 1-2, when the displacer piston is at the top of the stroke, the power piston is at mid-stroke.

In order to improve the efficiency, the engine requires a heat regeneration system. Such a system, which we call a regenerator, is used to temporarily store heat energy so we can add it back later. A regenerator can be any material that conducts heat and can allow air to flow through, such as wire mesh or honeycomb structures. When the air flows from the hot side to the cold side the air is sent through the regenerator, which pulls heat energy out of the airflow. This energy is stored in the regenerator rather than being lost on the cold side. Reversely, when the air

flows from the cold side back to the hot side, the energy stored in the regenerator is put back into the airflow, so less energy needs to be replaced by the hot side.

### Overview of Liquid Piston Stirling Engines

Liquid piston stirling engines operate on the same principle as kinematic stirling engines, but with two main differences. First, liquid pistons replace the mechanical pistons. Second, the pistons can no longer be connected to one another physically and must be set linked by frequency rather than physical linkage. When replaced with a liquid piston, the displacer piston becomes a liquid filled U-tube with one side of the U-tube heated and the other side cooled. Likewise, the power piston is replaced with a column of liquid that can respond to the pressure changes in the engine, as seen in Figure 1-3. In Figure 1-3a the displacer liquid has been shifted so that the majority of air in the engine is on the cold side. As a result, the pressure drops in the engine drawing the power piston in and decreasing the height of the liquid in the output tube. In Figure 1-3b the displacer liquid has been shifted so that the majority of the air is on the hot side. As a result, the pressure increases in the engine and the power piston is pushed out, increasing the height of the liquid in the output tube.

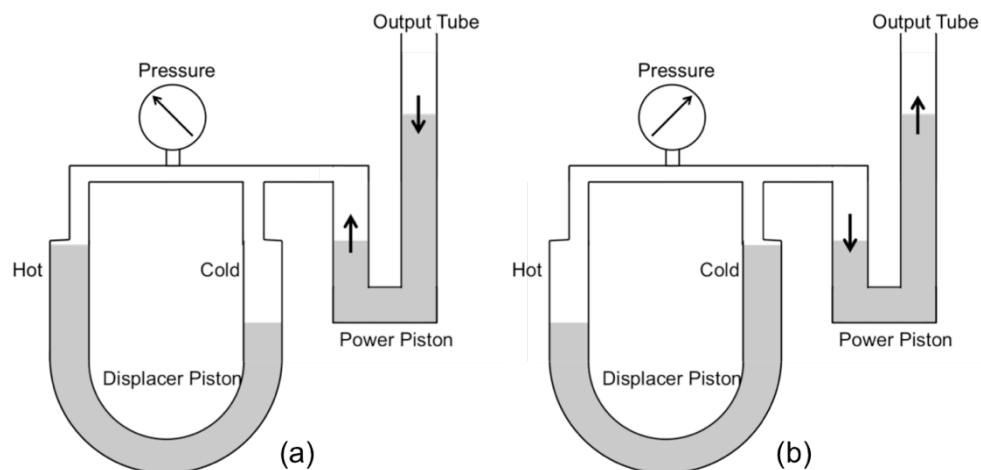


Figure 1-3: Displacer and power piston action in an LPSE

Because the two pistons cannot be physically linked, their movement has to be linked by frequency. In order for the movement of the displacer piston to be 90° out of phase of the power piston they must both move at the same natural frequency, which must also match the frequency of the pressure variations in the air. Matching the frequencies of the LPSE components is called tuning and is an important design consideration.

While kinematic stirling engines must transfer the mechanical power output from the power piston to drive a pump, liquid piston stirling engines can directly pump water in the output tube. Using one-way check valves, water can be drawn into the engine through one valve when the pressure is low, like in Figure 1-3a, and when the pressure is increased, like in Figure 1-3b, the engine can pump water out through the other valve. LPSE designs similar to this will be designed and modeled in this study.

### **Overview of TRACE Thermal-Hydraulic Code**

TRACE (TRAC/RELAP Advanced Computational Engine) is a thermal-hydraulic code developed by the NRC (Nuclear Regulatory Commission) for the purposes of modeling nuclear reactors. The code was developed to work with SNAP (Symbolic Nuclear Analysis Package), a graphical interface software package with pre-processing and post-processing abilities. TRACE has the ability to model multidimensional two-phase flow, transient thermodynamics, heat transfer, and fluid dynamics.

SNAP takes a component-based approach to modeling thermal-hydraulic systems, meaning that each component of a reactor is modeled individually and then connected. Components are selected and connected visually in SNAP, which then initiates TRACE code when executed. TRACE solves the two-phase flow and heat transfer partial differential equations with a finite volume numerical method and solves heat transfer equations with a semi-implicit

time differential method. After processing, SNAP's plotting features allow for data analysis by selecting parameters at any of the component cells throughout the model.

TRACE was chosen as the modeling code for its strengths in modeling thermal-hydraulic systems and its visual interface through SNAP. Because LPSEs are complex two-phase engines with thermal considerations and complex fluid dynamic behavior, TRACE is one of the few developed codes that can adequately model its behavior. SNAP's visual interface and post-processing abilities allow for easily made changes and fast data analysis.

### **Research Goals and Approach**

Compared to liquid piston stirling engines, kinematic stirling engines are more extensively researched and developed. The purpose of this paper is to advance the understanding of liquid piston stirling engines and enable future researchers to further improve the design and operation of LPSEs. Modeling LPSEs in TRACE thermal-hydraulic code allows researchers to analyze the effect that design and operation changes have on engine performance. The visual interface in SNAP allows for quick design changes and post-process plotting allows for easy data analysis. By validating the modeling technique for LPSEs in TRACE/SNAP, future researchers have an easy method to optimize and test LPSE designs without constructing physical models.

This paper details work done to validate the modeling technique. Chapter 3 explains the process used to design a functioning LPSE to be modeled in TRACE. Chapter 4 shows how I validated the TRACE modeling technique by modeling each component of the LPSE individually. The modeling and testing process for the LPSE designed in Chapters 3 and 4 is detailed in Chapter 5. To prove validity, Chapter 6 models and tests two documented, physical LPSE designs to confirm their behavior. Finally, Chapter 7 concludes the paper by summarizing results, conclusions, and lessons learned.



## Chapter 2

### Review of Relevant Literature

The basis for a large portion of today's liquid piston stirling engine technology research and development comes from the work conducted in the late 1970s and 1980s. Working for Oak Ridge National Laboratories, C.D. West drew upon his and Professor Graham Walker's kinematic stirling engine experience to develop the basis of liquid piston stirling engine research. West's work on liquid piston stirling engines included the many of the governing heat transfer equations, design guidelines, and operating profiles still used today.

For computer modeling of liquid piston stirling engines there three topic areas of previous research to be reviewed: (1) analysis of liquid piston stirling engines, (2) design of liquid piston stirling engines, and (3) mathematical modeling and simulations of liquid piston stirling engines. Table 1 summarizes previous literature of these topic areas. My research distinguishes itself into a fourth topic area, because it is the first effort to use a thermal-hydraulics code on a graphical interface, finite volume solver.

**Table 3-1: Summary of previous research**

Topic Area	Researcher (s)	Reference	Topic	Analysis / Design /Model	Equation Based Model / Computational Thermal-Hydraulic Model	Graphical Interface
1	C.D. West et al.	1,2,3,4,5	Fluidyne Equations of Motion, Experiments, and Analysis	Analysis	N/A	No
	G. Walker et al.	6	Experiments with Displacer and Tuning Line	Analysis	N/A	No
	Van De Ven et al.	7,8,9	Liquid Piston Stirling Engine Optimization	Analysis	N/A	No
2	C.D. West	1	Design Guidelines for Fluidyne Engines	Design	N/A	No
	M.J. Elston et al.	10	Design and Testing of Prototype Engine	Design	N/A	No
	F. Kyei-Manu and A. Obodoako	11	Design and Testing of Prototype Engine	Design	N/A	No
3	L. F. Goldberg	12	A Computer Simulation Mathematical Model of Liquid Piston Stirling Engines	Model	Equation Based Model	No
	M. Ozdemir and A.F. Ozguc	13	Mathematical Model of Fluidyne Engine	Model	Equation Based Model	No
4	Andrew Kriebel	N/A	Modeling Liquid Piston Stirling Engines in Thermal-Hydraulic Computational Modeling System	Model	Computational Thermal-Hydraulic Model	Yes

### **Liquid Piston Stirling Engine Research**

Dr. West has several publications about liquid piston stirling engines, analysis of their operation, and evaluations of their feasibility [1,2,3,4,5]. In his work, West defines the governing equations for stirling engine operation based upon an engine's piston stroke length, volumes, temperatures of hot and cold sides, mean pressure, and operating frequency. West explains the basis for liquid piston stirling engine operation relies on the fact that air expands when heated or, when confined, rises in pressure. This pressure change, which is responsible for power output, is triggered by moving the air in an engine between hot and cold spaces. Therefore, the functionality of a liquid piston stirling engine relies on maintaining the oscillation of air between hot and cold side, which is caused by the oscillation of the fluid in the engine. Designing the engine is critical because sustained operation requires the frequency of operation to match the natural frequency of the engine. Liquid piston behavior and the sizes of components such as diameters and lengths of tubing determine the frequency. Just as many researchers have done since West, I will rely heavily upon West's analysis and mathematical relations to model and analyze liquid piston stirling engines in my research.

West has published his research efforts that cover many areas of liquid piston stirling engine analysis, optimization, design, and development. The largest source of this information comes from "Liquid Piston Stirling Engines," a culmination of analysis, previous designs, and design guidelines [1]. His other papers, before and after this book, include an analysis of factors affecting engine operation, dynamic analysis of the engine motion, phase analysis of displacer motion, and documentation of possible uses in solar powered irrigation pumping [2,3,4,5]. In conjunction with G. Walker, O. Fauvel and other researchers, West develops the groundwork that most other researchers either built upon or were inspired by. Some of the few working on liquid

piston stirling engines with West, G. Walker and O. Fauvel also contribute to this groundwork as co-researchers on tuning line behavior [5,6].

In more recent years, stirling engines and liquid piston stirling engines have received additional attention from researchers and engine developers. Citing many of West's published reports, James Van de Ven and his team of researchers at Worcester Polytechnic Institute have been working to improve LPSE performance by focusing on heat transfer and gas compression improvements [7,8,9]. In his works, Van de Ven investigates the benefits of LPSE technology and methods to achieve operation closer to the high theoretical efficiency of the stirling cycle. One method is to create near-isothermal operation to increase engine efficiency by decreasing engine dead space. Because liquid pistons can conform to any volume, the heat exchangers can be designed with larger surface areas and smaller dead volumes. This increases efficiency by eliminating waste heat, bringing operation closer to the isothermal processes of the stirling cycle. Van de Ven also suggests using inlet and outlet valves as a method to control flow and bring operating volume changes closer to the theoretical stirling cycle profile.

### **Designing and Testing Liquid Piston Stirling Engines**

When discussing the design of liquid piston stirling engines, the first name to be mentioned, once again, must be C.D. West. In conjunction with his mathematical analysis of the dynamic motions of LPSEs, West also details his efforts in designing and testing physical engines. His book, "Liquid Piston Stirling Engines," is notable for the depth in which it details the design process for liquid piston stirling engines [1]. In this book, West not only discusses the engines he has built and tested, but also discusses how to design and build similar engines. In my research, I have found that many developers since cite these design guidelines as the basis for their designs. As many before me have done, I relied on these guidelines for building and

analyzing the models I have made. In fact, I chose one engine design documented by West to model and test in this paper. West covers displacer design, tuning line design, pumping design, heating requirements, dead volume analysis, flow losses, heat transfer losses, and effects of evaporation.

Around the same time as West, a team at University of Witwatersrand in Johannesburg, South Africa were also developing and designing useful liquid piston stirling engines for pumping water. The team of researchers, named here as M. Elston et. al, document the efforts to design a liquid piston stirling engine [10]. Beyond this documentation, however, the results of their experimentation and development is limited.

Finally, one design team at Swarthmore, which is later focused on in this paper, document a design project to develop a solar powered liquid piston stirling engine pump [11]. The team, consisting of F. Kyei-manu and A. Obodoaku, follows the design guidelines documented by West. Unlike other design efforts, the Swarthmore team provides depth and detail into their design process, prototyping, testing, and results. For this reason, I chose to use their engine as one that I have modeled and tested.

### **Mathematical Models and Simulations of Liquid Piston Stirling Engines**

Although the dynamics of liquid piston engines have been the focus of previous research efforts, as Van de Ven suggests, there is a need for a computer model of a liquid piston engine. Previous efforts to model the behavior of LPSEs have been based around mathematically derived equations of motion. These equations of motion take into account a thermodynamic analysis similar to the governing equations West described in his work. These models are simplified with assumptions about geometry or liquid piston behavior. One effort to model the operation of a liquid piston stirling engine was conducted by L.F. Goldberg in 1979 at University of

Witwatersrand in South Africa [12]. Goldberg simulates the cyclical response and behavior of a LPSE by observing the pressure, temperature, volume, and power fluctuations over time.

Goldberg's analysis relies on inputted second and third order equations of motion in a mathematical solver.

More recently, Ozdemir and Ozguc developed a more complex model of LPSE behavior [13]. Ozdemir and Ozguc's mathematical model considers the system as three parts: liquid, vapor, and interfacial regions. The interfacial region where evaporation and condensation occurs separates the liquid pistons and vapor working fluid. In their model, the liquid phase is responsible for the majority of the major and minor losses and the vapor phase behaves isentropically. Both of these phases are assumed to be open systems, because heat exchange occurs in the interfaces. Solving the mathematical system of equations, Ozdemir and Ozguc conclude that their model agrees with behavior seen in previous studies and the major and minor losses in the system are too great to produce appreciable output power. Ozdemir and Ozguc solve their simulation with the Runge-Kutta method in a mathematical solver.

### **Differentiation and Conclusion**

Building on the progress of previous researchers, advanced computer models are the next step in the advancement of liquid piston stirling engines. Modeling engine designs is crucial for the development of successful designs and advancement of the field because it allows for easy changes and analysis. Future researchers need reliable computer modeling methods to test and optimize designs without spending extra time and money on physical prototyping and testing. Previous researchers have identified this need. Van de Ven points out the need for advanced computer models and other researchers have attempted this, but with limited success, because the models still require considerable work to establish design relations and equations of motion.

Mathematically derived inputted second and third order equations of motion require advanced planning and solving methods, each of which have limitations. Often these simulations require assumptions to solve that can cause shortcomings. With advancements in computing power and modeling codes, there has been a need for newer modeling techniques for liquid piston stirling engines. Additionally, researchers need a modeling platform that is easy to learn, use, and widely available.

This paper aims to solve these problems. TRACE thermal-hydraulic code was developed for nuclear reactors and has strengths in modeling the behavior of two phase flows with dynamic behavior and heat transfer. For this reason, it is an attractive option for modeling liquid piston stirling engines. TRACE is a finite volume computational system similar to other fluid dynamic and heat transfer solvers. Because TRACE is built onto the SNAP graphical interface platform, it adds extensive pre-processing and post-processing capabilities as well as improved user interface. This allows for quicker modeling, easy design changes, and the ability to monitor parameters like pressure, velocity, water level, mass flow, and heat transfer at any finite volume in the model.

For these reasons, my efforts differentiate themselves from previous researchers' works. Never before have liquid piston stirling engines been modeled in a thermal-hydraulic code, especially one designed for two phase flows with dynamic behavior and heat transfer models built in. Additionally, TRACE differentiates itself as a finite volume computational system. Perhaps a more distinguishing aspect of my method is the use of a graphical modeling interface with pre and post processing abilities. While previous researchers have used inputted second and third order equations of motion with mathematical solvers, SNAP is an easier, quicker, and more user friendly platform where models are built graphically and equations are compiled by the system. Modeling liquid piston stirling engines with TRACE and SNAP is a new method using a thermal-hydraulic code, finite volume solver, and graphical interface. A validated modeling technique will prove a useful modeling tool for future researchers with wide appeal.

## Chapter 3

### Designing a Liquid Piston Stirling Engine

This chapter will detail the design of a theoretical LPSE given the design guidelines provided by C.D. West in his book *Liquid Piston Stirling Engines* [1]. Throughout the design process, several assumptions are made to simplify calculations and design choices. The first assumption is that this design will function and operate as a liquid piston stirling engine, although this is not necessarily true. Designing to guidelines does not ensure that the engine will function. One purpose of developing a computer model is to allow easier testing of potential LPSE designs.

One major goal of this experimentation is to advance the development of LPSEs for water pumping in developing regions of the World. As a goal, we will aim to pump  $1 \text{ m}^3/\text{hr}$  to a head of 2 m, which is large enough to serve a small irrigation system. In order to maintain simplicity, this machine will use water as a piston fluid, air as a working fluid, will operate at a mean pressure close to atmospheric, and the design will favor standard sizes wherever possible. Additionally, we will assume the hot side will be heated by solar energy to a hot side temperature of approximately 600K and the cold side will be maintained around 300K.

For our design, we will chose a liquid feedback design, which has a tuning column of water coming off from the displacer cylinder that serves to add power to the compression stroke when the raised liquid column from the expansion stroke returns to a lower level. Like the power piston, the tuning column must be designed so that its natural frequency matches the frequency of the displacer piston. The design is set up to pump water as the power piston is coupled into a pumping configuration with two one-way valves. This design can be seen in Figure 3-1.

Our design guidelines provided us with a few design parameters. First, for most conveniently sized LPSEs, the frequency is usually around 0.5 – 0.7 Hz [1]. We will aim to

design an operational frequency of around 0.6 Hz. Second, if we are to pump  $1 \text{ m}^3/\text{hr}$  to a height of 2 m, we are able to calculate the necessary power output from the engine.

$$\text{Power } W = \dot{V} \rho g h$$

$$W = \left( \frac{1 \frac{\text{m}^3}{\text{hr}}}{3600 \frac{\text{s}}{\text{hr}}} \right) \left( 1000 \frac{\text{kg}}{\text{m}^3} \right) \left( 9.81 \frac{\text{m}}{\text{s}^2} \right) (2 \text{ m}) = 5.45 \text{ W}$$

Knowing these parameters, as well as the temperatures and mean pressure, we can begin to design the engine.

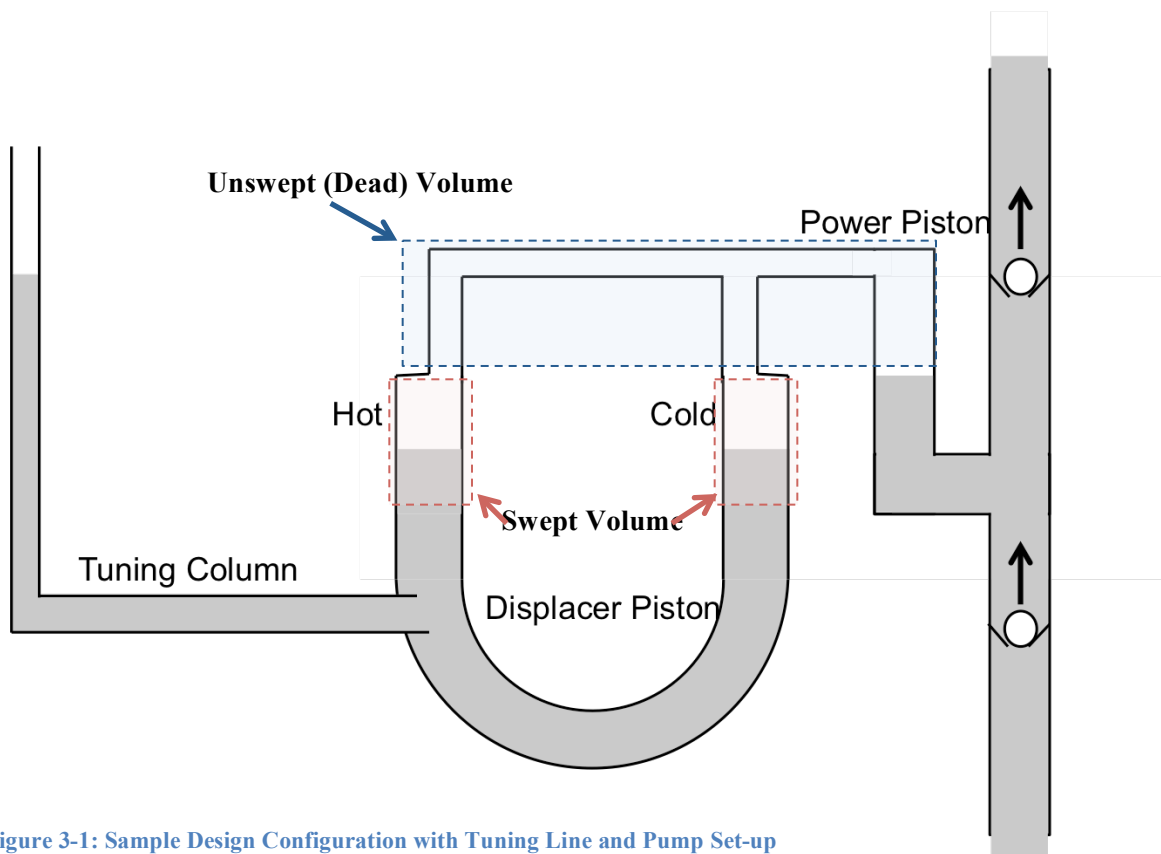


Figure 3-1: Sample Design Configuration with Tuning Line and Pump Set-up



### Displacer Design

The frequency of displacer piston oscillation is a function of piston length. According to West, to solve for displacer length for a 0.6 Hz frequency [1]:

$$L_{disp} = \frac{g}{2\pi^2 f^2}$$

$$L_{disp} = \frac{9.81}{2\pi^2 (0.6^2)}$$

$$L_{disp} = 1.38m$$

Knowing the power output of a stirling engine we can estimate the necessary swept volume using a simple relation that includes the Beale number, which is a performance characterization of stirling engines [1].

$$W = B_n P f V_o$$

For an engine with a hot side temperature of 600K, a typical Beale number is around 0.005 [1]. We have estimated pressure to be about 100kPa, frequency to be around 0.6 Hz, and work needed to be approximately 5.45 W. Knowing these parameters, we can calculate the necessary swept volume for an engine.

$$V_o = \frac{W}{B_n P f}$$

$$V_o = \frac{5.45W}{(0.005)(1 \text{ bar})(0.6 \text{ Hz})}$$

$$V_{o_{disp}} = 0.001817 \text{ m}^3$$

Since our design attaches the tuning line between the hot and cold sides, the hot and cold pistons will behave closer to a 90-degree phase difference. This means that although the total volume change is 1817 cm<sup>3</sup> each piston only needs to displace each stroke  $\frac{V_o}{\sqrt{2}} = 1285 \text{ cm}^3$ .

Generally, West states, the stroke length and diameter of the cylinder should be equal [1]. Since

the swept volume of a piston is equal to the cross sectional area multiplied by the piston stroke length. We can calculate the diameter and stroke length with the equation:

$$V_{disp} = 0.001285m^3$$

$$V_o = \frac{\pi d^3}{4}$$

$$\left(4 * \frac{0.001285 m^3}{\pi}\right)^{\frac{1}{3}} = d$$

$$d = 0.118m$$

If we are to use standard material choices such, as PVC for the low temperature tubing, it would be convenient to use a standard size, such as 5in tubing, which has an inner diameter of 0.127m.

$$d_{disp} = 0.127m$$

To calculate the piston stroke length:

$$\left(4 * \frac{0.001285 cm^3}{\pi(0.127m)^2}\right) = s$$

$$s_{disp} = 0.101m$$

### **Dead Volume**

For a configuration like this one, West states that the optimum compression ratio occurs when the un-swept volume available is 1.12 times larger than the swept volume in the cylinders [1]. So for this design, the un-swept volume is:

$$V_{US} = 0.001439m^3$$

If the frequency is 0.6 Hz, there are 2160 cycles per hour. Since our volume flow rate goal is 1 m<sup>3</sup>/hr, we must pump 0.000463 m<sup>3</sup> per stroke. In our design, the pumping piston is gas-

coupled to the engine with an air filled pipe (see Figure 3-1). This means that when the system is at rest  $0.000463/2 = 0.000231 \text{ m}^3$  of air and  $0.000231 \text{ m}^3$  of water must be present in the pumping piston system. Subtracting this dead volume from the total volume, we now have  $0.001208 \text{ m}^3$  left of dead volume for the engine space.

$$V_{pump} = 0.000231 \text{ m}^3$$

As an approximation,  $1/4$  of this remaining volume will be used for connections and clearances, leaving  $3/4$  of this remaining volume for the heat exchangers. For optimization, it is suggested that the regeneration space should be about twice the size of the heater space [1]. This yields the following volumes:

$$V_{connect} = 0.000302 \text{ m}^3$$

$$V_{Heater} = 0.000302 \text{ m}^3$$

$$V_{regen} = 0.000604 \text{ m}^3$$

### **Tuning-Line Design**

Given the design parameters including the adiabatic volume (hot cylinder, pump, connectors), isothermal volume (cold cylinder, regenerator, heater, and connectors), displacer diameter, and the operating frequency, West states that it is possible to relate the tuning-line length and diameter with the following equation [1]:

$$L_{tl} = 2252 D_{tl}^2 + 0.69$$

From this equation we can populate a table of possible tuning line designs, using common piping and tubing diameters.

Table 3-1: Possible Tuning Line Configurations

Diameter, mm	Length, m	Volume, L
25.0	2.1	1.0
32.0	3.0	2.4
40.0	4.3	5.4
50.0	6.320	12.4
65.0	10.2	33.9

Since our machine has a total swept volume of 1.8 L, we can right away eliminate diameters of 25mm, 32mm, and 40mm, because the 1.8L stroke would represent too much of the total volume of the tuning line. We can also relate sizes based on friction losses. Friction losses for a 65mm diameter tube are about half that of the 50mm tube. Both of these factors call for larger diameter tuning-lines, as does the need to limit acceleration of liquid pistons to prevent splashing. However, as the diameter increases, so does the length of the tuning-line. To keep the length of the tuning line to a reasonable size, we will select a 50mm diameter, 6.3m length tuning-line.

$$D_{tl} = 0.050m$$

$$L_{tl} = 6.320m$$

### Insulation, Connections, and Heat Transfer

If designing a physical machine, great care would be made to design optimum conditions for operation. For one, efforts would be made to limit evaporation from the hot cylinder using an insulating float. This float would limit evaporation by limiting the surface area between the hot air and the liquid piston, but would add additional dead volume and shuttle losses. Additionally, design modifications would be made for the hot cylinder to behave adiabatically, and for the cold

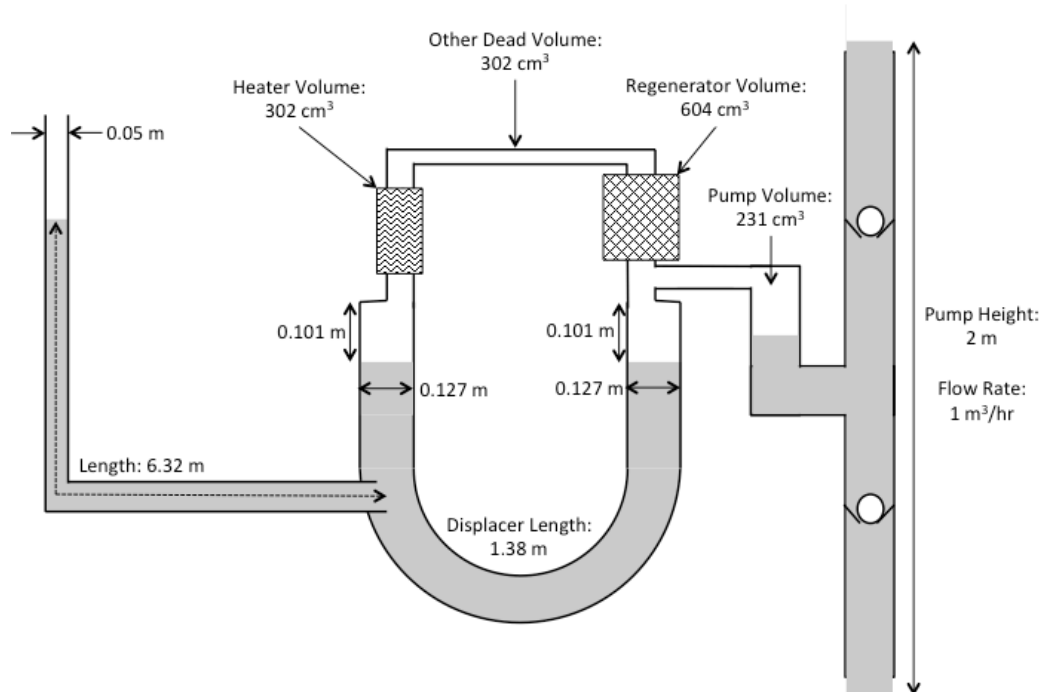
cylinder, heater, and regenerator to behave isothermally. Since we are designing a machine for testing in TRACE, less care has to be made around these designs. Through TRACE, parts of the engine can be modified to represent adiabatic and isothermal conditions. Likewise, evaporation can be limited by designing the liquid-air interface to mimic the effects of an insulating float. For this reason, designs for these components will not be stressed in this chapter.

### Summary of Design Decisions

A summary of design decisions made can be seen in Table 3-2 and Figure 3-2

**Table 3-2: Design Summary**

Cold-cylinder stroke	0.101 m
Cold-cylinder diameter	0.127 m (isothermalized)
Hot-cylinder stroke	0.101 m
Hot-cylinder diameter	0.127 m (adiabatic)
Displacer length	1.38 m
Tuning-column length	6.32 m
Tuning-column diameter	0.05 m
Pump mean volume	231 cm <sup>3</sup> (half pumping stroke)
Regenerator internal volume	604 cm <sup>3</sup> (isothermalized)
Heater internal volume	302 cm <sup>3</sup> (isothermalized)
Connector and dead space volume	302 cm <sup>3</sup> (1/3 adiabatic, 2/3 isothermal)
Heater Temperature	327° C
Cold-cylinder Temperature	27° C



**Figure 3-2: LPSE Design Configuration**

### **Ideal Power Output**

For our purposes of estimation, the ideal power output of our engine can be estimated with through the Schmidt analysis [1]. For the calculation, we will assume the following parameters:

Fluid type:	Air
Mean Pressure:	101 kPa
Heater Temperature:	600K
Cooler Temperature:	300K
Phase Lag:	90°
Clearance Volume:	10 cm <sup>3</sup>
Cylinder Swept Volume:	1285 cm <sup>3</sup>
Heater Volume:	302 cm <sup>3</sup>
Regenerator Volume:	604 cm <sup>3</sup>

Using an extended version of the Schmidt analysis, the calculated power is approximately 42 J per cycle, or 25 W. This calculation runs on the approximation that the heaters, coolers, and regenerator behave isothermally, however if we calculate for an adiabatic hot cylinder the ideal power is closer to 23.8 W [1]. This number assumes that the hot and cold cylinders will operate with a 90 degree phase difference. This theoretically yields the highest ideal power, but losses decrease with increasing phase angle making phase angles between 90 and 120 reasonable as well.

## Flow and Heat Losses

One challenge in modeling in TRACE is approximating the losses in the system, as TRACE has no losses by default. All system losses will have to be estimated and represented by loss coefficients in the different finite volumes. As far as flow losses, we are concerned with viscous losses and kinetic losses and the main source of flow losses will come from the tuning line, which is the longest component in the system. Keep in mind, general estimates are all that are necessary. Since TRACE/SNAP does not allow for great accuracy in modeling losses, and instead only offer loss coefficients, there is little need to calculate losses with great accuracy.

West explains that from previous examples we can expect viscous losses to detract about 10% of the ideal output from system. This equates to about 2.4 W of loss. Similarly, we can expect kinetic losses to detract about 7% of the ideal output from the system [1]. All together this is about 4 W of flow losses in the tuning column alone. While loss estimates for the tuning line have better accuracy due to the size of the line, displacer and pump arm losses are extremely rough estimates. From previous work, it can be expected that these two will combine to detract about 20% of the ideal output power [1]. For our purposes, we will assume that our system will lose around 5W due to the pump and displacer.

Finally, one of the most important losses is the transient heat transfer loss in the hot cylinder. In calculating the transient heat transfer loss you must first know the pressure variation amplitude. For a 600K engine and 90 degree phase difference this is approximately 40.8 kPa from peak to peak [1]. This will be useful later in analyzing the engine cycles. From this we can determine the total transient heat transfer loss. This loss decreases dramatically with increasing phase angle. At a 90 degree phase angle, the expected loss would be approximately 12W, but be could be lowered to around 7W at an 120 degree phase angle [1]. For our approximation, we will assume a 9W loss.

Normally, in designing an engine, calculations are stressed to find the necessary input power to maintain isothermal conditions in the heater and regenerator. Because TRACE allows for components to be set as isothermal, these are not necessary worries in modeling an LPSE. For purposes of estimating total power losses though, we can estimate that heat losses necessitate that input power be approximately 300% higher than ideal [1].

Totaling flow losses and heat transfer losses, the approximate loss from ideal is around 18W. Leaving our system with approximately 5.8 W of output for useful pumping. From our earlier calculation, this is enough to reach our pumping goal. However, as previously explained the losses are very rough approximations. In modeling, my goal will be to mimic losses similar to these. Every physical system has very different losses due to its construction. For our modeling purposes where we include losses as loss coefficients, these rough estimates are sufficient. In summary, I will modify losses the model until the output amplitude is approximately 20-25% of the amplitude without losses.



## Chapter 4

### Validation of Modeling Technique Using Discrete Components

Before modeling an entire engine, it is advantageous to break down and model individual components of the engine. By modeling and testing the performance of individual components, I can validate the modeling technique and validate that the design behaves as it should. The more components that are connected, the harder it will be to study the behavior of a single component, therefore this technique simplifies the modeling process. Additionally, each step of modeling components individually will reveal the modeling settings necessary for reliable results. It is important to note that this technique will validate the individual components, but is not sufficient validation for the entire engine.

#### U-Tube Displacer Piston

Mirroring the design process of Chapter 3, the first component to model will be the displacer piston in the U-Tube. This component modeling validates the calculations relating displacer piston design to operational frequency. This model will be designed as a simplified

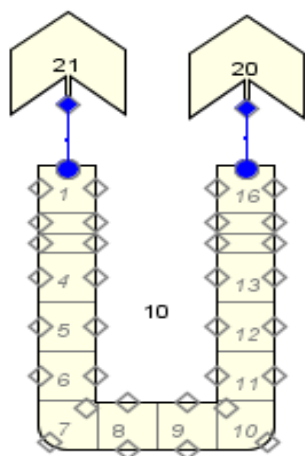


Figure 4-1: SNAP U-Tube Design

version of the displacer piston designed in Chapter 3. Using the same length (1.38m), diameter (0.127m), and stroke length (0.101m) the model seen in Figure 4-1 was designed as a TRACE object in SNAP. The design features a pipe component divided into 16 cells. When designing this component in SNAP, you must set the size and orientation of each cell to reflect the desired design. In this design the smaller cells (2,3,14,15) are the areas that will be swept by the cylinder

surfaces. As our system will be operating with water and air, the model is set to treat liquids as water and non-condensable gases as air. At the opening of each end of tubing, break components act as an opening to atmospheric conditions.

To start we need to get the system to a steady state. Setting the gas fraction of cells 1, 2, 15, and 16 to 1.0, they are set to be gas while the rest of the cells are water. This represents the system at rest with both pistons at mid-stroke. By running a steady state calculation, we allow any incorrect initial conditions to work out and save conditions when the system is truly at rest. These steady state conditions can now be saved as the new initial conditions for this model.

In order to set the system into oscillation, the initial conditions are modified so that one piston is at top dead center and the other at bottom dead center. To see the affects of this on the system, a transient calculation is run. Because the initial conditions are slightly off due to the change in water level it is useful to place the initial step size to -1.0 s. This allows for slight recalculations in initial conditions before starting the problem time.

Running the transient calculation for 20s, the interesting parameters to evaluate are gas volume fraction in the swept volume area and velocity in the bottom of the u-tube. These parameters can be seen in Figures 4-2, 4-3, and 4-4. As it can be seen, these parameters vary in a harmonic pattern of a certain frequency. Additionally, the two sides of the u-tube operate at a 180° phase shift, which is to be expected. By calculating the time between peaks in the cycle, the frequency of operation was calculated to 0.57 Hz. This is roughly a 5% error to the designed frequency, which is within the expected frequency variation [1]. With this information, we can validate to a reasonable degree that SNAP/TRACE can be used to accurately model the frequency behavior of oscillating fluid in a u-tube.

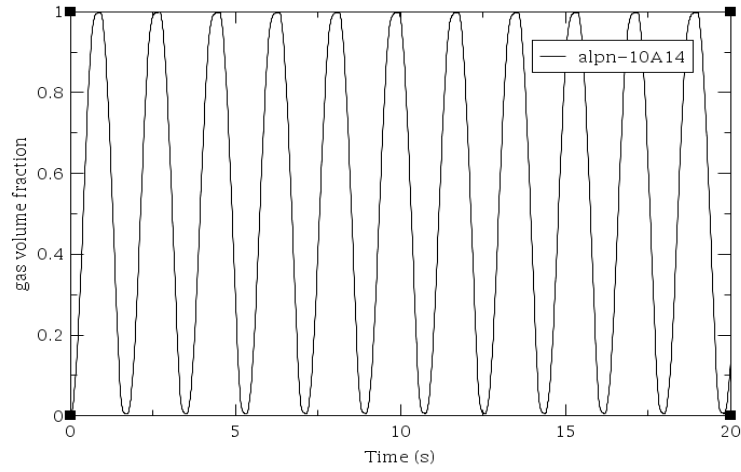


Figure 4-1: Gas fraction of right side showing cylinder height change harmonically

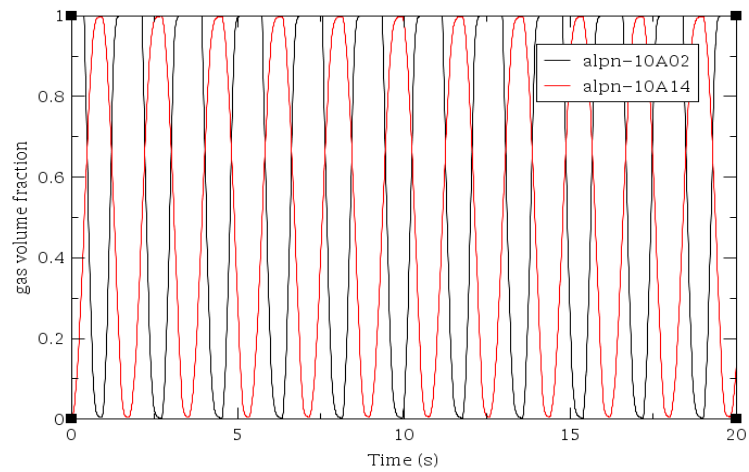


Figure 4-2: Gas of left side (black) to right side (red) showing 180 degree phase shift

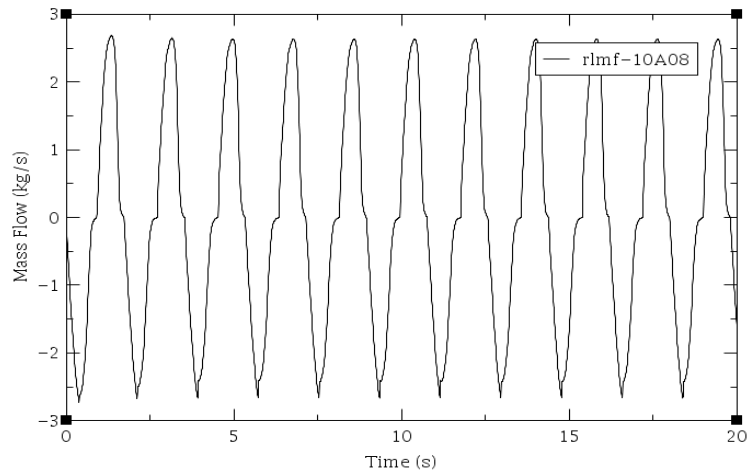


Figure 4-3: Mass flow measurements in middle of u-tube

As seen in the transient calculation shown, there are no losses present in this model. This is fine for calculating frequency, but before moving forward it is important to confirm that friction losses can be incorporated into the model. By adding friction calculation abilities to the model and adjusting the friction factor values for the u-tube the once sustained oscillations now decrease in amplitude over time eventually coming to rest. At this point, the exact frictional values are not important, but confirming frictional effects in the model allows us to move forward with further modeling.

### **U-Tube Displacer with Tuning-line**

Having confirmed the frequency behavior of oscillating fluids in a u-tube, a tuning-line can now be added to the system. Once again, we are looking to observe that the frequencies of the displacer and tuning columns behave as expected. In order to do this the model becomes increasingly complicated. Rather than one pipe as a u-tube, the u-tube is now made up of two pipe components and one tee component. This can be seen in Figure 4-5. The cells of these components are adjusted to have the same orientation, angles, lengths, and diameters as the u-tube they are collectively making up. From the tee connection (1/5 of the way from the hot side to cold side in the displacer), the tuning line is directed away from the u-tube before being turned up to form the tuning column [1]. Once again the initial conditions are set to decide what is liquid and what is air. In this part of the process, particular care has to be made to ensure that the resting level of the tuning line is the correct ‘length’ distance from its entrance into the u-tube. In our case this is 6.32m with a 0.05m diameter. Additionally, ensure that the column height is enough to accommodate the entire swept volume stroke. The final major design change is that instead of the displacer ends opening to atmospheric they will be now connected with an air tube with the dead volume of 1439 cm<sup>3</sup>.

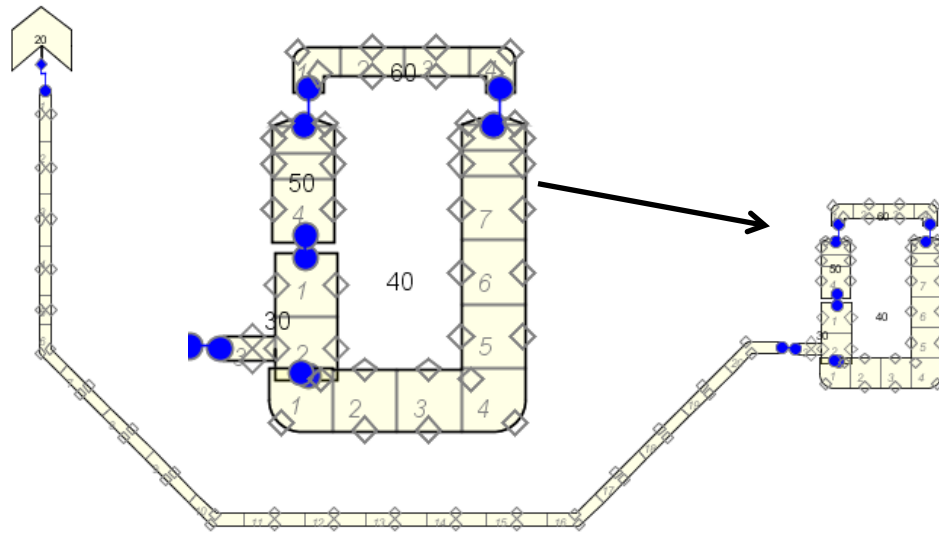


Figure 4-5: SNAP model for U-Tube with Tuning Line

Even though the engine is designed to have pistons operate at a  $90^\circ$  phase difference, this will not occur until the heating elements are added so that gas pressure fluctuates. Instead, in this experiment we will start with the tuning line at rest and excite the displacer piston into oscillation. As can be seen in Figure 4-6, the oscillation of the displacer and tuning line are at the same frequency of approximately 0.57 Hz. Additionally, it can be seen that as the tuning line amplitude increases the amplitude of displacer oscillation decreases. In this case, the tuning line level is being measured above rest. So a drop in gas fraction corresponds to an increase in tuning line height. In the displacer, this is the same. A drop in gas fraction corresponds to the level increasing above mid-stroke. From this we can see that left (hot side) of the engine operates in phase with the tuning line. Therefore, both the tuning line and hot side operate  $180^\circ$  out of phase from the cold side. This is what we ideally would see. Because more energy is added in the expansion stroke than is taken out during the compression stroke of the engine, the tuning line momentum adds energy to the compression stroke.

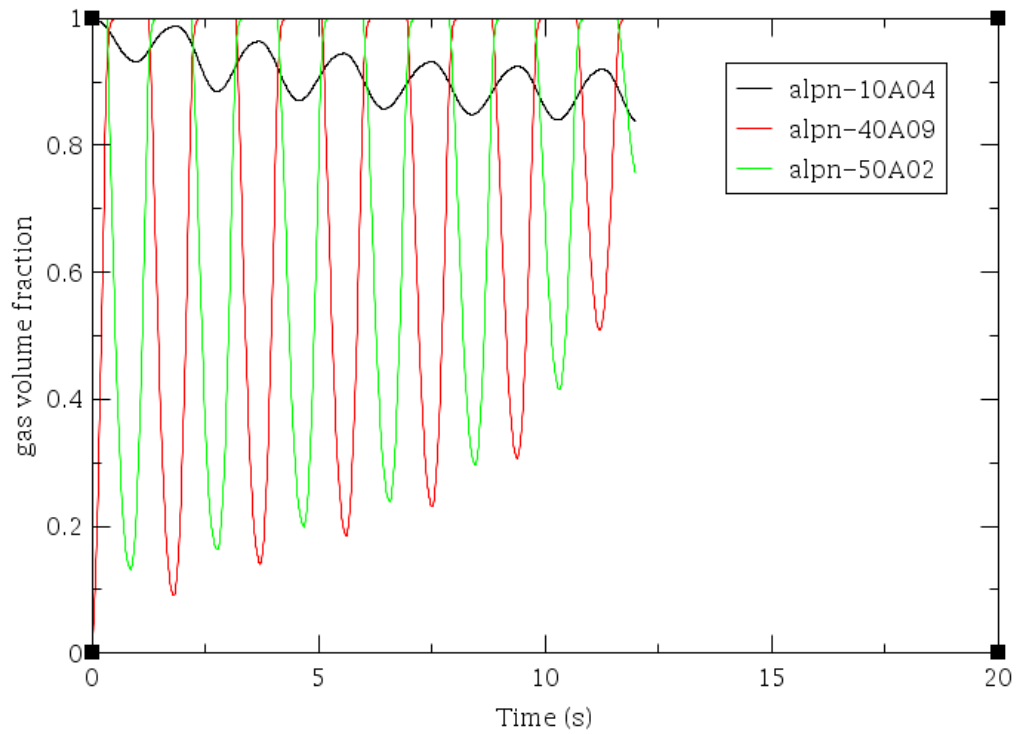
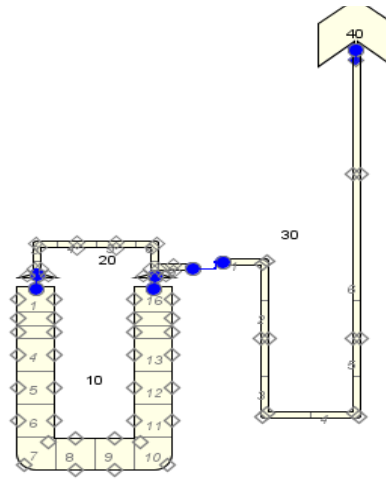


Figure 4-6: Oscillations of Tuning Line (black), hot side (green), and cold side (red)

### Heating and Cooling

Having confirmed the validity of the displacer and tuning line designs, it is now time to incorporate heating and cooling into the model. For this we will remove the tuning line from the u-tube, connect the air connection tube to a power piston u-tube, and add heater and regenerator space. From the design in Chapter 3, we can design with a dead volume of  $1439 \text{ cm}^3$ , of which  $604 \text{ cm}^3$  is regenerator volume,  $302 \text{ cm}^3$  is heater volume,  $302 \text{ cm}^3$  is connector volume, and  $231 \text{ cm}^3$  is pump volume. This design can be seen in Figure 4-7. As previously determined, the heater will be 600K and the regenerator will be 300K. For our purposes now, we can set the rest of the components to 300K isothermal as well.



**Figure 4-7: SNAP model with heating components and simple pump output**

The power output here is just a smaller u-tube with liquid at the bottom. As pressure fluctuates in the engine, this will show pressure fluctuations in the form of water level changes in the output tube. One imperfection of this is that without designing this u-tube to match the same frequency of the displacer, the pressure fluctuations will not be harmonic as it will be affected by the momentum of this pump u-tube and the temperature changes. Despite this, we can validate this portion of the model if we see that oscillating the displacer causes temperature and pressure fluctuations in the engine.

With the heater element in cell 1 and the regenerator in cell 16 (volumes determined by changing average flow area), the displacer is set to oscillate. There are three parameters of interest: temperature in the air connection, water level in the output column, and pressure in the air connect. These parameters can be seen in Figures 4-8, 4-9, and 4-10, respectively. In Figure 4-8, we can see that temperature varies in a consistent pattern approximately between 360K and 310K. These temperature changes started changes in the level of the water in the output column, which can be seen to vary periodically in Figure 4-9. Finally, both the temperature changes and momentum of the output column affect the pressure in the air connector. As a result, in Figure 4-10 pressure variations between 106 kPa and 104 kPa can be observed at multiple frequencies.

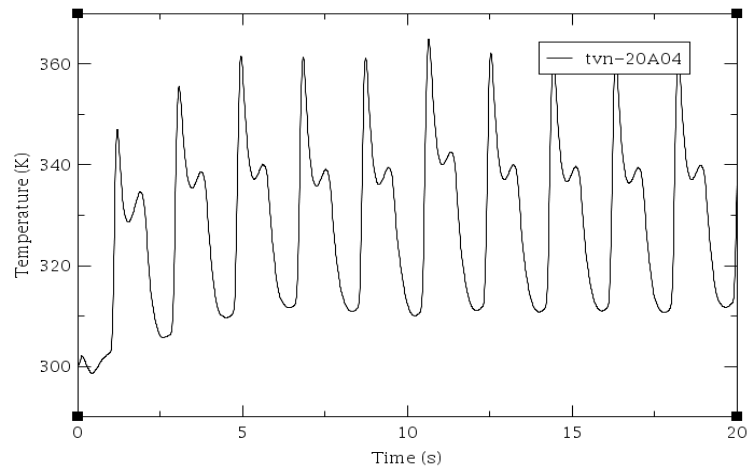


Figure 4-8: Temperature fluctuations in the air connection tube

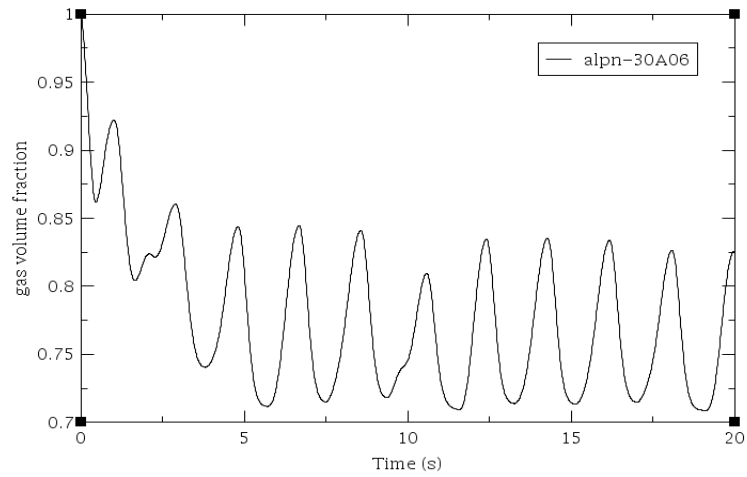


Figure 4-9: Water level changes in the output tube

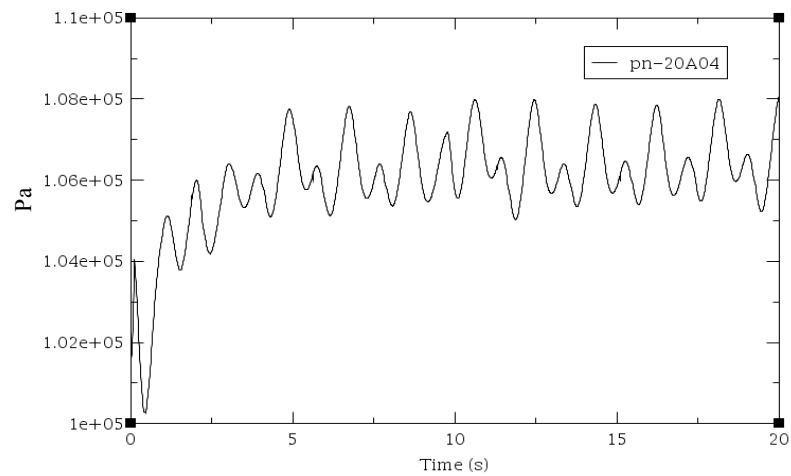


Figure 4-10: Pressure Fluctuations in the air connection tube



From the results, it can be seen that the water level changes and pressure variations in the air connection tube are a result of the oscillating system sending air through the heater, regenerator, and cooling components. While the system was not designed exactly how it would be if we would construct an engine, it has proved that TRACE/SNAP can accurately model how oscillation in the u-tube with temperature elements can cause pressure changes and head output.

### Simple Pump Setup

Now knowing that we can create pressure oscillations with the previous setup, we need to determine whether we can model a simple pump in SNAP/TRACE that can be driven by pressure oscillations. Shown in Figure 4-11, the pump model consists of two one-way check valves (denoted by hourglass symbols) connected by a tee-pipe. The main line of the tee creates the pumping line, the side tube comes off and then is angled up to create the pumping arm where we will apply the pressure oscillations. The bottom check valve is placed at the bottom of the u-tube

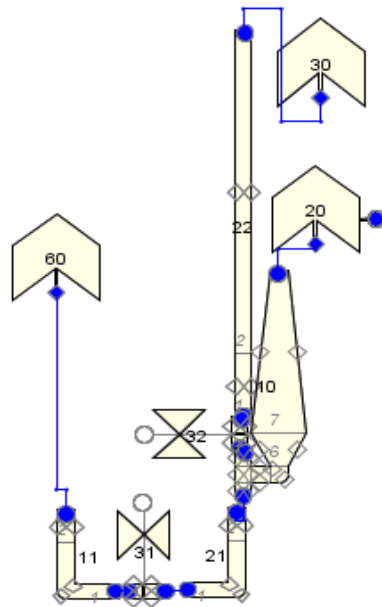


Figure 4-11: SNAP Pump Model

to simulate being placed below the water level. Above the upper check valve a long tube extends with two cells, one that is initially water, the second initially dry that allows for easy tracking of water level increase. Due to issues with the pumping arm emptying itself, the diameter of the pumping arm was increased to allow for a greater volume of water. All breaks are at atmospheric conditions. However the bottom break is liquid, and the pump arm break is set to oscillate +/- 60000 Pa at 3 second increments.

When a 30s transient calculation is run on the model, the results are less consistently periodic than we are used to seeing so far. The valve models add a level of complication that causes problems with bringing the system to steady state. As a result, even though pressure oscillations are delivered smoothly from the pump arm break, the resultant pressure changes have a larger amount of noise. Seen in Figure 4-12, the noise from the check valves can be seen as the disruptions along the smoother waveform. Despite the noise, the pumping action is still evident. In Figure 4-13, the mass flow of the two check valves are plotted showing when each valve opens to allow fluid through. As it can be seen, the two valves alternate opening and closing as water is pumped in and out with the pressure oscillations. This pumping action results in changing the water level in the output line and the pumping arm. In Figure 4-14, the gas fraction of the pumping arm in red and the output line are plotted. This plot shows the pumping arm increasing water level periodically with the pressure drop, then lowering level as the higher pressure pushes the water up to the output line. This can also be seen in the output line, as each time the pumping arm lowers water level the output level increases. This is the pumping action we are interested in. In this case the maximum water level appears to approach a gas fraction of 0.65, which in a 1m tube is 0.35 m. Overall the pumping system here as a maximum head of approximately 0.6m.

All in all, this simple model confirms that SNAP/TRACE can be used to model a simple pump. Although there are additional complications with the check valves, the pumping concept can clearly be seen. This experiment validates the last crucial component to the LPSE pump model. Additionally, this experiment identifies the need to carefully model the pumping system to minimize potential complications.

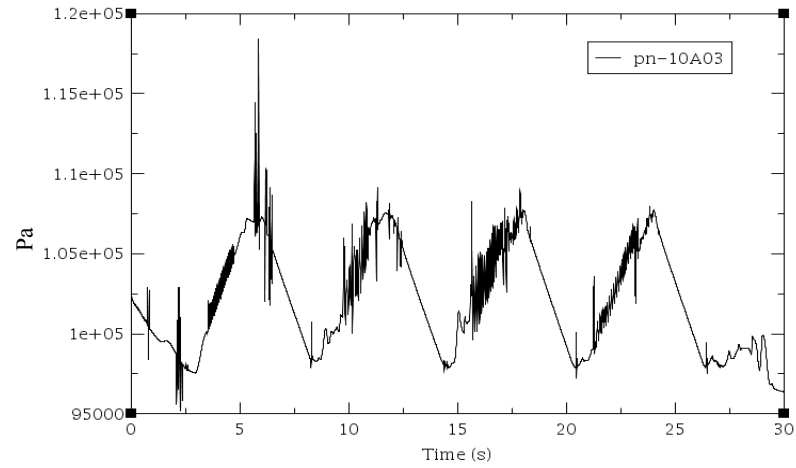


Figure 4-12: Pressure Fluctuations in the tee

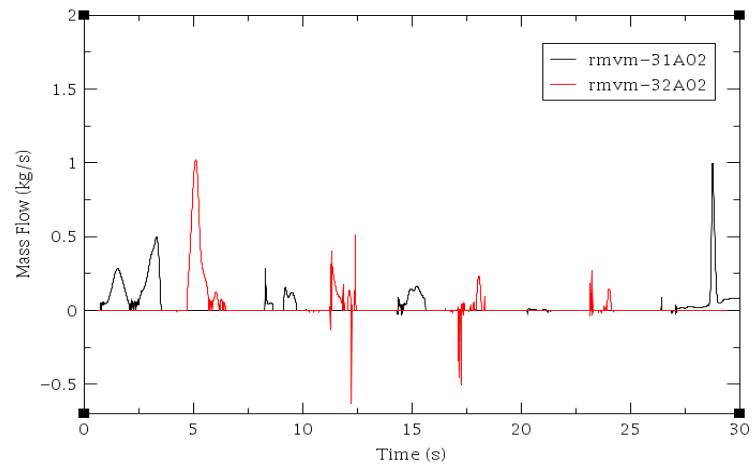


Figure 4-13: Mass flow through bottom (black) and top (red) check valves

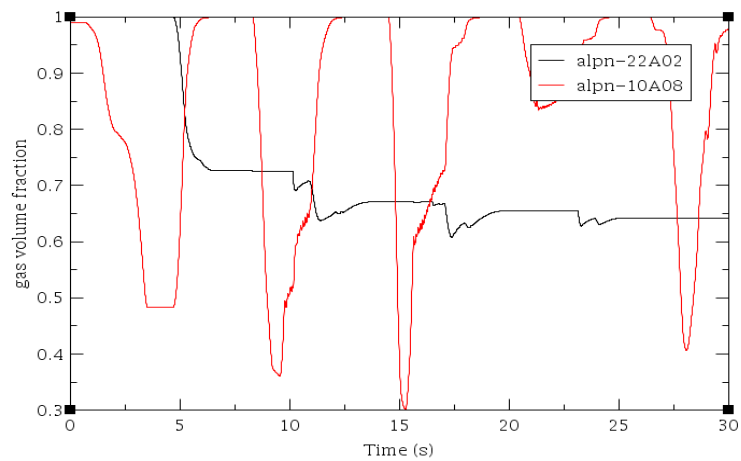


Figure 4-14: Water level changes in pumping arm (red) and output tube (black) represented by gas fraction

## **Chapter 5**

### **Liquid Piston Stirling Engine Modeled in TRACE**

This chapter explains the process for modeling the designed LPSE in TRACE. Using the previous component models that have been tested individually, the engine will be modeled and pieces will be added throughout the process. Throughout the modeling process, the model will be adapted to fit the design guidelines and to improve performance. Additionally, attempts are made to make the engine similar to how it would be made physically, while also trying approximate isothermal/adiabatic assumptions. As previously stated in Chapter 3, it is important to remember that while the engine was designed around mathematical relations and experimental guidelines for engine performance, there is no guarantee that the engine functions as expected or that it even operates.

#### **Displacer U-Tube and Tuning Line**

Using the design constraints and previous models, the displacer u-tube will be made of three components: hot cylinder, cold cylinder, and u-tube tee. The two cylinders are only the size of the swept volume and the u-tube is the connector with a tee-line to attach the tuning line. From previous experiments we have shown that this component operates close to expected and oscillates close to the natural frequency.

The hot cylinder is made of pipe component with a diameter of 0.127m divided into two equal parts of 0.0505m (total length 0.101m). By dividing this component into two cells at the mid-stroke line, it is easy to set initial water levels and track oscillation. As previously discussed, the hot cylinder is approximated at adiabatic, so this component will not include calculations for

heat transfer across the pipe wall. This component should be modeled as a vertical pipe as it would be in the physical setup. To start the initial conditions of the pipe are at atmospheric conditions with the top half of the cylinder filled with air and the bottom half with water.

The cold cylinder is physically similar to the hot cylinder. The swept volume portion of the cold cylinder is 0.101m in length and divided into two equal cells. However, to accommodate for the diameter change going into the pipe above, a third cell is added to the top that is 1mm in length that will be the cone-shaped nozzle where the diameter change takes place. Also, the cold cylinder will be modeled as isothermal at the cold-side temperature. To do this, the component needed to include pipe wall calculations. This means turning on the pipe wall model with the pipe walls very thin (0.1mm) and cooling the outside of the pipe with a liquid of with a high heat transfer coefficient and low temperature (300K). Inside initial conditions are set similar to the hot side, so the top half is air and the bottom is water.

The u-tube portion is very similar to previous designs. Using a tee component, the main line should be 1.279m in length and 0.127m in diameter. This gives the appropriate displacer length of 1.38m. The tee line should be 0.050m in diameter and length is relatively unimportant, but 0.1m is good for this design. In order to improve loss calculations, this component is divided into 10 equal length cells. To make the 'U' shape, the cell orientation is at the appropriate joints. Approximately, the tee should tuning line should enter 1/5 of the way from the hot to cold length (3<sup>rd</sup> cell) [1]. In our design, this component is adiabatic so the pipe wall calculations are turned off. The initial conditions for now are set at atmospheric with the entire tube filled with water.

The tuning line is very similar to how it was designed in Chapter 4. The line is modeled with a pipe component that is greater than 6.32m in length and is 0.05m in diameter. To aid in the prevention of errors in component length junctions, the pipe is broken into 16 cells. Although the shape is not crucial, it is important that the tuning line is turned from roughly horizontal to vertical the same height that it enters the u-tube. From there the cells extending vertically should

be set to lengths so that the initial height of the water is at the same resting height as the cylinders. For now initial conditions are set to atmospheric with all cells below the water level set to water and those above set to air. One end of the tuning line connects to the tee from the u-tube, the other side is attached to a break component set to atmospheric conditions in air to represent where the system is open to the surroundings.

### **Dead Volume Components**

The dead volume of the engine is broken up into four components: heater, hot side connector, regenerator, and cold side connector. In this portion of the engine, diameters and flow areas of the components vary between components. Additionally, the lengths and orientations of these components are critical, as they will form a closed loop with the u-tube cylinders (for now).

The heater element of the engine is where all heat input will occur. For simplicity, the outer diameter is the same as the hot side cylinder, so they can be in the same physical pipe. In reality the heater would be a resistive element inside with the air flowing around it. The design for a solar heated heater would be more complicated. To design for an inner resistive element we will assume a 3.5mm annular gap between the element and the wall, with a length to a 302cm<sup>3</sup> volume. We will model this with three cells, two within the heating area and one 1mm length cell to act as the cone nozzle as we did with the cold cylinder. We are assuming this component is roughly isothermal at the hot-side temperature of 600K, so we will model the pipe wall as very thin and surrounded by a high heat transfer fluid of 600K. The initial conditions are set to atmospheric air for now. This component connects to the top of the hot side cylinder and the bottom of the hot side connector.

The regenerator element is similar to the heater element in its design. It is designed as an annular regenerator with the air flowing around a heat storage material in the middle. This is once

again modeled as a pipe with an 0.127m outer diameter and a reduced flow area to account for a 3.5mm annular gap. To account for the 604cm<sup>3</sup> designed volume the length must therefore be twice the length of the heater. This component is assumed to be isothermal space as the gas temperature leaving the regenerator should be the same (heat added when cold air enters or heat removed when hot air enters). To model this the pipe wall calculations are turned on and the pipe walls are modeled with larger thickness without heat transfer to the surroundings. This way when the pipe walls reach the operational temperature the heat capacity of the walls keeps the component at a steadier temperature. Initial conditions are set to atmospheric air. This component attaches the hot side connector and the cold side connector. For this design, it is useful to bend the regenerator into an L-shape so that neither connector needs to be longer than necessary to close the loop. Since both ends of this component connect smaller diameter connectors, we will model the regenerator in 5 cells, where the two outer cells are the nozzle/diffusers that are very short in length and the three middle cells are the regenerator where the middle cell has the bend.

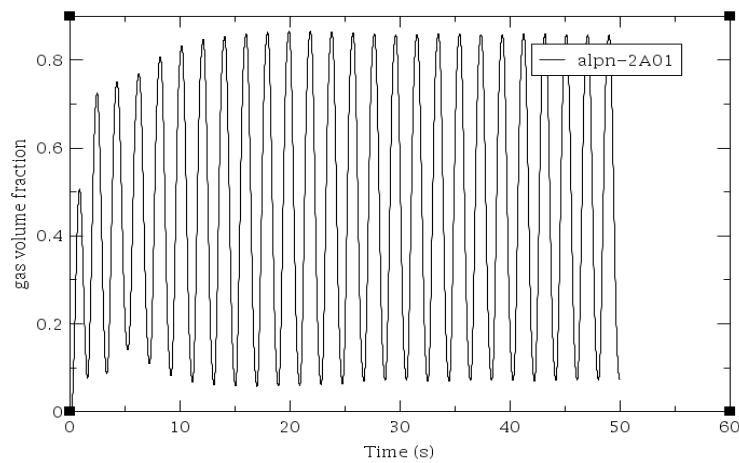
The two connectors along with the pump connection make up the rest of the dead volume of 302cm<sup>3</sup>. Previously, we estimated that 1/3 of this volume should be assumed to be adiabatic while the rest is isothermal. As roughly 2/3 of the connection volume is needed in this portion, we will model the connectors as isothermal and the pump connections as adiabatic. For now, we will leave out the pump connections from the model to keep a closed system in the engine.

The hot side connector connects the heater to the regenerator and must be the correct length to do so. The cold side connector connects the regenerator to the cold side cylinder. Knowing the lengths of the components, the diameters must be set so the volume of the connectors are correct. The hot side connector will be L-shaped, so it can connect the heater and regenerator. Therefore it is modeled with three cells with the middle cell containing the bend. The cold side connector is a straight pipe and is therefore only modeled with 1 cell. The pipe walls are

both set to moderate thickness to store heat in the pipe walls. Like other components, initial conditions are set to approximate atmospheric air.

### Testing the Setup

Upon completing the design setup, setting preliminary initial conditions, and thermal settings, the next step is to correct initial conditions by running a steady state calculation. Running the steady state calculation, a sign of success appeared, as the system that was initially at rest did not reach steady state, but instead began to oscillate. The oscillations in the hot cylinder can be seen in Figure 5-1, as the water level drops in the cylinder with increasing pressure in the air space causing oscillations to build as the tuning responds. This occurrence indicates that the engine with the liquid feedback tuning line does indeed self-start into oscillations. Therefore to calculate steady state initial conditions the heat structures must be turned off.



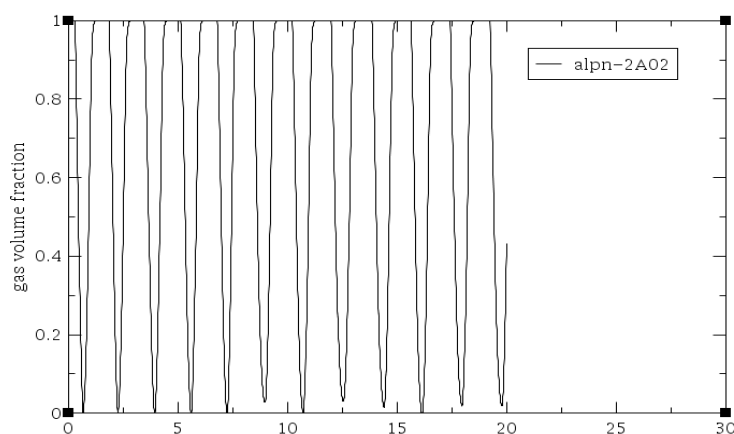
**Figure 5-1: Oscillations occurring in the Hot Cylinder**

The simplest way to turn off heat structures is to remove pipe wall calculations from all components so that no energy is added to the system. In this state, a steady state calculation can be conducted. When the system has reached steady state the calculation will stop and by saving



results in the Job Status window, the steady state conditions can be loaded into initial conditions in the model options.

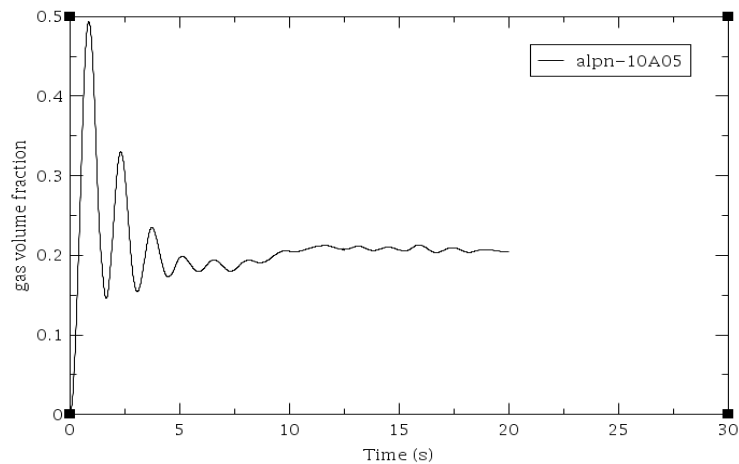
Now that the model has proper initial conditions, it is important to confirm that the model behaves properly. We have already proved with the steady state calculation that with no heat added, the system remains at rest. The next step is to observe what happens when the system is set into oscillation without friction. By offsetting water levels in the hot and cold cylinders to top and bottom dead center respectively, the system is now unbalanced and will oscillate when released. By running a transient calculation, we can observe that the system oscillates freely and indefinitely as seen in Figure 5-2.



**Figure 5-2: Free Oscillations in the Hot Side Cylinder with no friction**

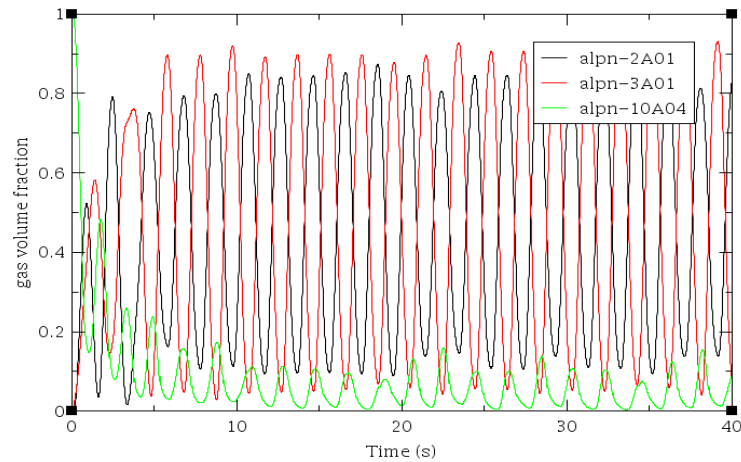
Obviously, a realistic system is not friction free. To turn on friction calculations turn on friction, wall drag, fluid friction, and gas friction in the Nameslist Variables in the Model Options. Then for each component add friction coefficients at cell boundaries. From experimentation, a 0.1 friction coefficient for all components nicely replicates the earlier calculated decrease to 20-25% amplitude. Additionally, to aid calculations, all cell junctions where a large flow volume change occurs must be flagged with an abrupt area change. With friction now in place, the system is once again set into unbalance and let to oscillate. Unlike

before, the system now oscillates in decaying amplitudes as seen in the tuning line oscillations in Figure 5-3. It is important to note that friction will never bring the system fully to rest in TRACE, but will decay amplitudes until they are reasonably negligible.

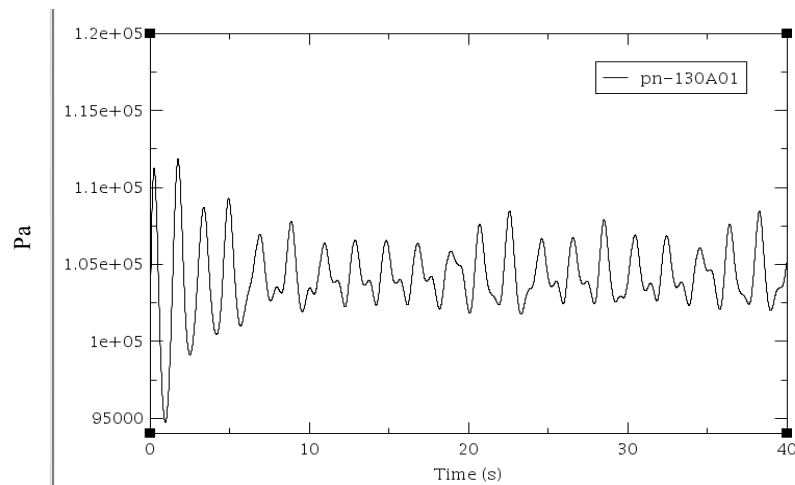


**Figure 5-3: Oscillations in Tuning line damped by friction**

Now that we have confirmed that the system comes to rest with friction, it is time to observe what happens when the system starts at rest and the heating elements are turned on. To do this, reset the water levels to previously determined initial conditions and turn on pipe wall calculations that include the heat structures. Running a transient calculation, we can once again observe how the system initially at rest, begins to oscillate. The oscillations build to high levels at first, before settling into a more consistent nature. Oscillations in the cylinders and tuning line can be seen in Figure 5-4 and also in pressure variations in Figure 5-5. The frequency of the engine is close to the natural frequency of the system. However, the phase angle of the cylinders is not how we expected, the hot and cold cylinders are  $180^\circ$  and the cold cylinder is  $180^\circ$  out of phase with the tuning line. This is more or less how it should function, but we expect closer to a  $90^\circ$  phase angle between the two cylinders. Also, we can see that the cylinders are not operating with a 0.101m stroke length, this is confirming what was expected while designing: the engine may not be fully functional just because the design guidelines were followed.



**Figure 5-4: Oscillations in Hot Cylinder (black), Cold Cylinder (red), and Tuning Line (green)**



**Figure 5-5: Pressure Oscillations in the engine show sustained oscillation with friction**

So, is this enough to confirm that the engine functions? Yes and no. For one, the system behaves as a heat engine. It shows that heat energy is converted into the motion of the system creating increased head in the tuning line. If we are only concerned showing that the principles of a liquid piston stirling engine are occurring, then yes, the engine functions. We can see that oscillations build causing oscillations in the displacer and tuning line and oscillating pressures. However, without the pumping line the system is not creating useful work and the phase angles of the cylinders is not quite right. We now need to add the pumping arm. Before doing so, the design of the working engine can be seen below in Figure 5-6.

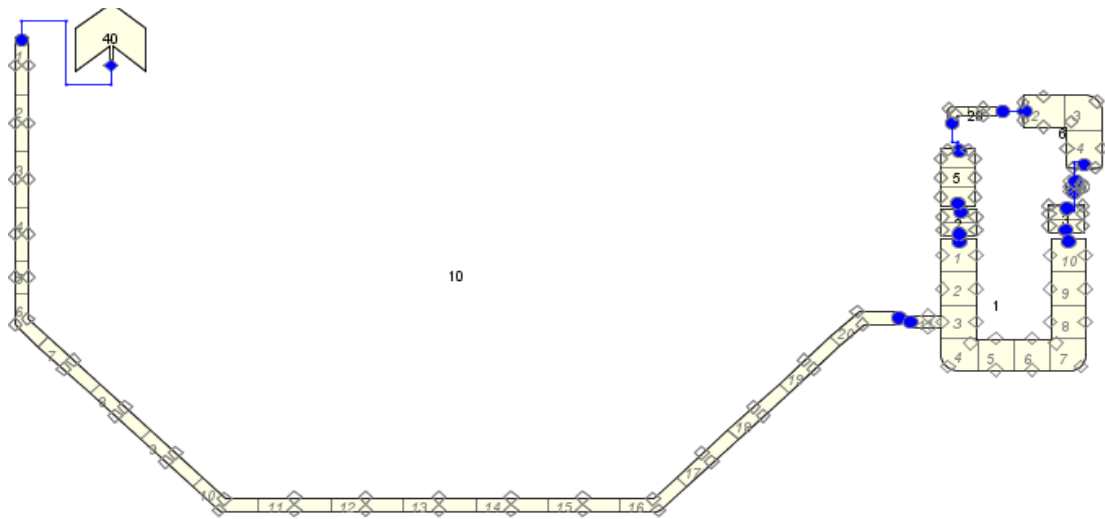


Figure 5-6: LPSE model before attaching pump arm

### Adding the Pumping Arm

As seen previously when testing the pumping setup, TRACE struggles with check valves in the system, so this is where problems are expected. To start we will set up a simple pump setup with very low elevation change. We know from our previous design, that the pump connection should make up the remaining  $101\text{cm}^3$  of dead volume and the pump should have  $231\text{cm}^3$  of air and  $231\text{cm}^3$  of water at rest. This is accomplished by changing the cold side connector to a tee component connected to the pump connection. The tee should have the main line the same size as the previous cold side connector and the tee line of 5mm in length and 2cm in diameter. The pump arm connection should be 0.194m in length with a 2cm diameter and should be bent to an L-shape to connect the horizontal tee to line to the vertical pumping area. Initial conditions should be set to atmospheric air. The tee component should be designed to isothermal conditions as previously explained and the connector should be adiabatic with pipe wall heat transfer turned off.

To allow more volume change with less elevation change in the pumping swept volume, the diameter the pumping arm should be larger. For this design I have chosen to go with a 4 cell pipe where the middle two cells are the swept volume with lengths of 4.86cm and 5.4cm diameters. To connect to the pump connector a short cell on top acts as a nozzle to change diameter, as done before. Additionally, the pumping arm is connected to the pumping line by having the bottom cell bend from vertical to horizontal. This component is set to atmospheric initial conditions where the top two cells are air and the bottom two cells are water.

Finally, the pumping line is composed of a tee connector with check valves above and below dictating the one-way flow. Above the check valves is the pumping line extending vertically and below is a feed line filled with water. The diameter of all these components is not entirely crucial, but from the previous design example a 5 cm diameter is sufficient. Once again, the lengths of these components are not crucial, but attempts should be made to ensure the system is at rest when pressure is constant and to minimize the pumping head as we do not expect the system to be powerful. The final design including the pumping arm can be seen in Figure 5-7.

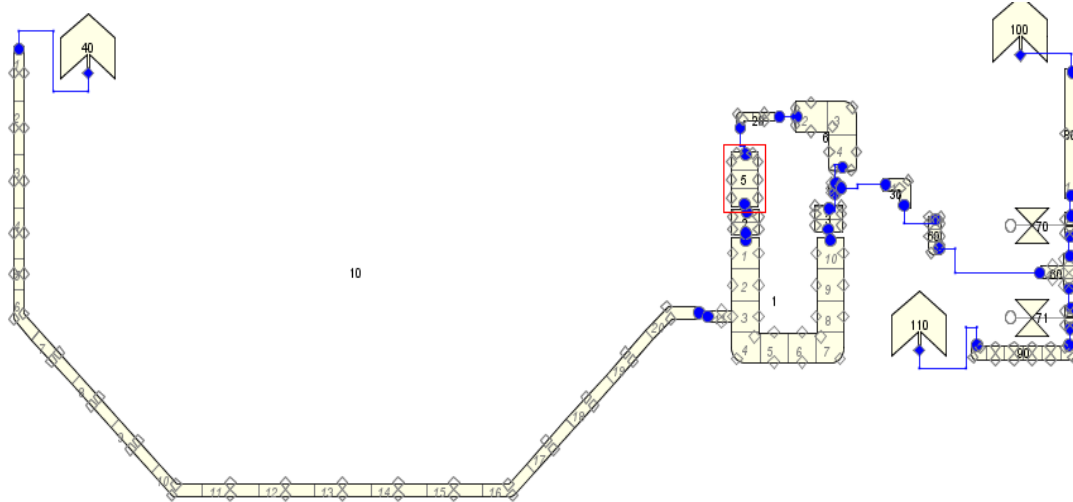


Figure 5-7: LPSE model with pump arm

### **Testing the Final Design**

With the system initially at rest and the heat structures engaged, as done before without the pumping arm, the system is set through a transient calculation. However, unlike before there are no sustained oscillations. In the first few seconds of the calculation, slight oscillations in water level can be seen as the displacer reacts to pressure changes faster than the pumping arm, however friction overcomes these oscillations as too much power is being put into the pump rather than the displacer. Therefore, oscillations stop in the system and pumping action stops after the water level changes in the pump to its maximum level for the new higher pressure in the engine. Pressure then is never lowered enough to draw water back into the pump as the pressure has built up too much without the oscillations to draw air into the cooler side of the engine. To make up for the lack of oscillation, tests were done to see what would happen if the system was set into oscillation to start. Once again, oscillations start, but are not continued and die out as friction overcomes the power added to the displacer.

These results are disappointing, but not entirely unexpected. Given TRACE's difficulties with the check valve models and without the guarantee that the LPSE design is functional, it is not surprising that the engine is not powerful enough to induce pumping. Despite the failure of the pump engine, tests without the pump attached validate to some degree TRACE's ability to model LPSEs and the validity of the design guidelines. Seeing how the engine without the pump self-started and sustained oscillations shows the functionality of the LPSE concept and shows that TRACE can be used to model this behavior. At this point, we have shown how to design an engine, how to test components in TRACE, and how to model an engine in TRACE. To move forward, we will attempt to validate the modeling technique by replicating designs that have been physically constructed and are known to either marginally perform or fully function as LPSE pumps.

## **Chapter 6**

### **Modeling Validated Engine Designs**

While previous chapters detailed the design, modeling, and testing of an engine that has never been built and tested physically, this chapter covers the modeling and testing of two engines that have been physically built and tested. To some degree the modeling technique has already been validated, but since the engine design has never been validated physically it cannot be determined whether the failure of the engine in Chapter 5 can be attributed to the design or the model. Therefore, the purpose of this chapter is to validate the modeling technique by comparing the model testing results to the documented results of physical engines.

Two engines documented engine designs, will be modeled and tested in this chapter. The first is a successful liquid piston stirling engine pump designed and built in a laboratory setting by C.D. West and documented in Chapter 4 of his book “Liquid Piston Stirling Engines” [1]. The second is a less successful engine designed and built by two students at Swarthmore using the same design methodology used in Chapter 3 of this paper [11]. Less detail will be provided in modeling techniques for these models, but all components are similar to those explained in Chapters 4 and 5.

#### **West’s Laboratory Engine**

Constructed from copper and brass fittings, West’s laboratory engine is described as one of his earliest designs that has been used as a starting point and inspiration for other’s own engine designs. Unlike the design from Chapter 3, this engine is designed without a liquid feedback tuning line, without separate heating and regenerator spaces, and instead is just a displacer piston u-tube water-coupled to a pumping line. This design can be seen in Figure 6-1, with the only

modification made to the distance between check valves to more closely replicate lower pumping head described by West [1].

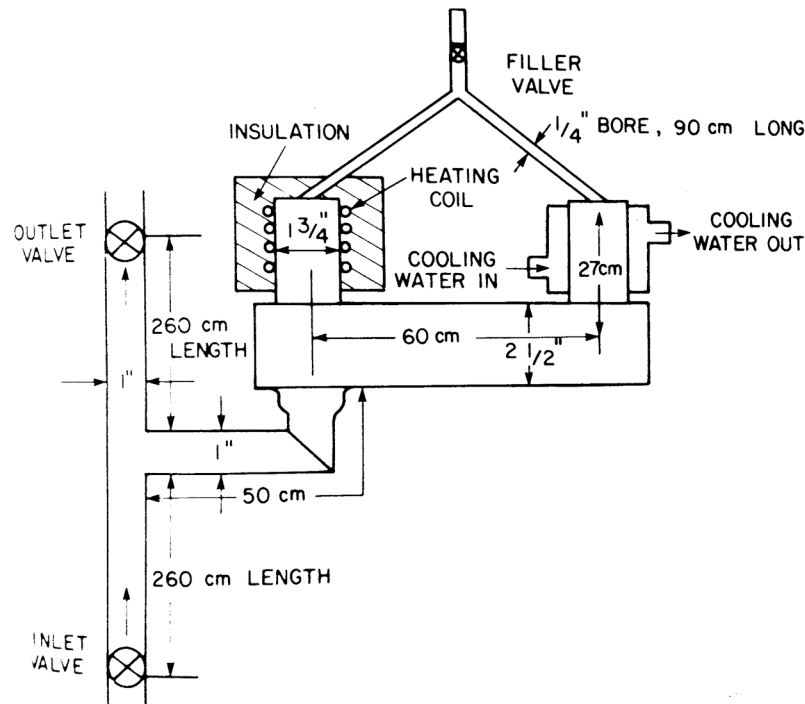


Figure 6-1: West's Laboratory Engine Design [1]

The engine design documented provides a reasonable amount of detail to model, however leaves some design decisions for junctions and overall layout. For modeling purposes, it is not necessary to have a filler valve, which would have been used to fill the displacer with water. Also, it is not necessary to model each separate pipe shown as individual components as TRACE/SNAP makes it possible to combine several of these components into the same pipe since we are not limited by standard pipe fittings. Limiting component junctions also aids with calculation speed and accuracy. It should be also noted that West's diagram is not to scale.

The first step is to design the displacer u-tube. This is accomplished by breaking West's u-tube portion into four components: the horizontal displacer tube, the cold side cylinder, the hot side cylinder, and the air connector. The horizontal displacer tube is documented to be roughly 60cm in length and 6.35cm in diameter. This is modeled rather simply with a pipe component that



is horizontal with a 90° bend at the far end where the tube turns up to connect with the cold side cylinder. The entirety of this part will be filled with water, so initial conditions were set to atmospheric water inside the pip.

The cold side cylinder is also rather simple to model with a pipe component. Subtracting the horizontal tube diameter from the 27cm distance shown in Figure 6-1, the cold side cylinder is a 4.45cm diameter pipe and around 24cm in length. The cold cylinder is where the cooling in the engine will take place and West indicates this is done with a cooling water jacket. To model this the pipe wall calculation is turned on, walls are set to a metal similar to copper/brass, and an exterior flow at roughly 280K is applied. For initial conditions, the bottom half of the cylinder is water and the top half is air.

To minimize the number of components the hot side cylinder is modeled as part of the tee component that connects the hot side cylinder, horizontal displacer tube, and pumping connector. This is done with a tee component where the main pipe length includes the tee and the entire hot side cylinder at 4.45cm diameter, and the side tee is necessary length so that the hot and cold side cylinders are 60cm apart. Initial conditions were set so that the water level in the hot side cylinder was at the same height as the cold side cylinder. Finally, turn on the pipe wall calculations in this component as this is where all of the heat will be applied.

Finally, the air tube connector is an extremely simple 0.64cm diameter and 90cm length tube that is bent to the right size so that it connects with the centerlines of the two cylinders. It was necessary to change the shape of the pipe to so that it connects to the cylinders from straight on. Since this design does not have a regenerator, this pipe is the closest thing to a regenerator, as a great deal of heat transfer occurs with the pipe walls as air oscillates back and forth. As a result, the pipe wall calculations should be turned on. Initial conditions should be set to atmospheric air.

Now that the u-tube portion is modeled, it is necessary to model the pumping components. To start, the pumping arm is a simple 50cm and 2.54cm diameter pipe that connects

the bottom of the hot side cylinder tee component and then bends horizontally to connect into the tuning line. This component is modeled with initial conditions so that it is filled with water.

Similarly, the pumping line is a simple tee component where both lines are 2.54cm in diameter. The height of the pumping line will be the pumping head for the system. While West, shows this as over 5m in the diagram, he indicates it is much less than this in successful tests. Therefore, the pumping line height is modeled between 1-2m in length and the side tee line is short and just necessary to make the connection to the pumping arm pipe. All of the pumping line is filled with water for initial conditions.

Above and below the pumping line are one-way check valves. These are modeled so that they are set to start closed and open when the pressure below them exceeds the pressure above them. To avoid some problems that were experienced in the past with high frequency vibrations in the check valves, the minimum position of the valve stem should not be set to zero. The check valves should have the same diameter as the pumping line and should be filled with water to start. The final components in the model are the breaks to atmospheric conditions. The bottom check valve should be connected to atmospheric water and the top check valves should be connected to atmospheric air.

The system is modeled as closely as possible to West's diagram, and can be seen in Figure 6-2. As has been done before, the initial conditions must be corrected by running a steady state calculation with all pipe wall conditions turned off. When the system has met steady state, the conditions are loaded into the initial conditions of the model. In preparation to run the transient calculation, the pipe walls can be turned back on, and the heating can be applied to the hot side cylinder. Knowing that West used a resistor heating element, the heater can be modeled either as a resistor with input power or as a heat structure with a set temperature. Either method can be used with success, however the input power method reaches unrealistic temperatures, so I have opted to go with a 600K heat structure.

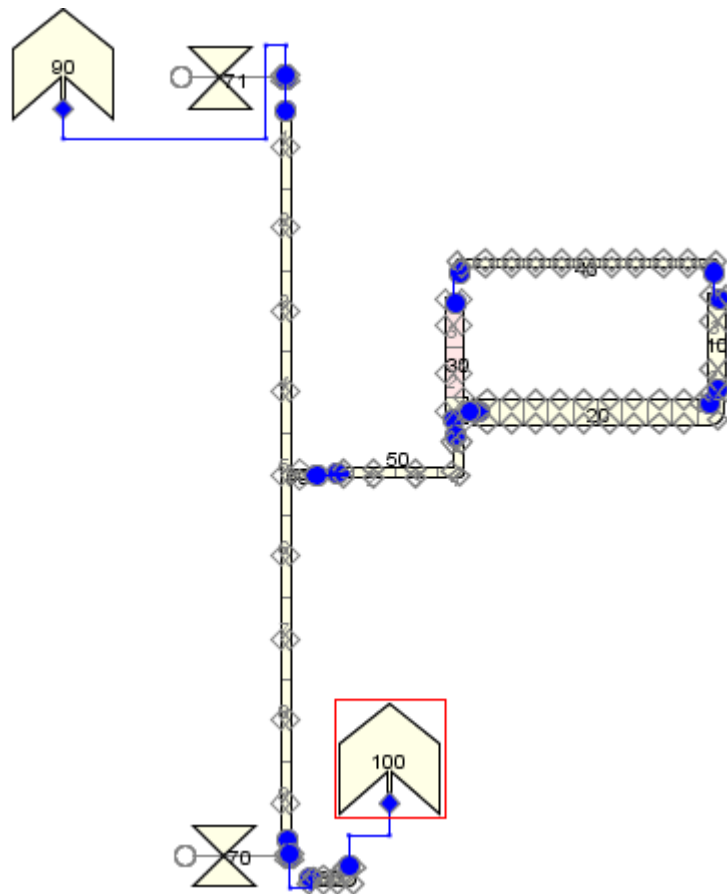
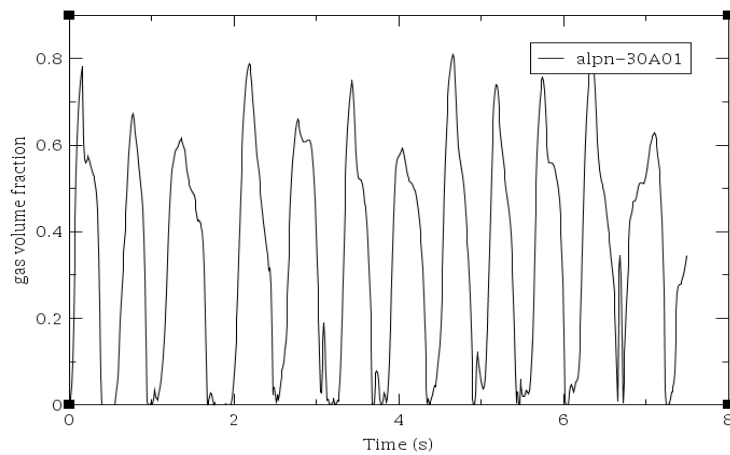


Figure 6-2: TRACE Model of West's Laboratory Engine

By running a 20 second transient calculation, we can evaluate the success of the design. In any component, it is obvious that oscillations are occurring in the system. Looking at the hot side cylinder, the water level oscillations can be seen in Figure 6-3. Without a tuning line it may be surprising to learn that the system is self-starting. In this type of engine, the system starts itself because a great deal of evaporation occurs at the hot side cylinder until pressure is built high enough to break the top check valve open. The water levels are then dropped as the pressure drops dramatically. This pressure drop condenses the evaporated liquid locally on the hot side creating a pressure difference between the two cylinders and starting the system into oscillation. These pressure changes can be seen in Figure 6-4, which shows the pressure oscillations in the air

tube connector. This effect is even more evident when using a resistor heater because the heater takes longer to heat up and cause the evaporation to occur.

The pressure oscillations in the engine are responsible for the pumping effect. When the pressure is high the top check valve opens and water flows up and out of the system. When the pressure is low the bottom check valve opens and water flows into the system. This pumping effect can be seen nicely in Figure 6-5, which shows the liquid mass flow through the check valves. The red line represents the top check valve and the black line represents the bottom check valve. Corresponding to large pressure spike when evaporation was occurring, the top check valve is the first to open to start the oscillations. From there the top and bottom check valves alternate back and forth as water flows out and into the system in cycles of roughly the same volume. By integrating the mass flow line of one peak and multiplying by their frequency, it can be estimated that the engine pumps roughly 500 L/hr. Which exceeds, but is still similar to West's estimate of 370 L/hr to 1.6m height [1].



**Figure 6-3: Water level oscillations in the hot side cylinder**

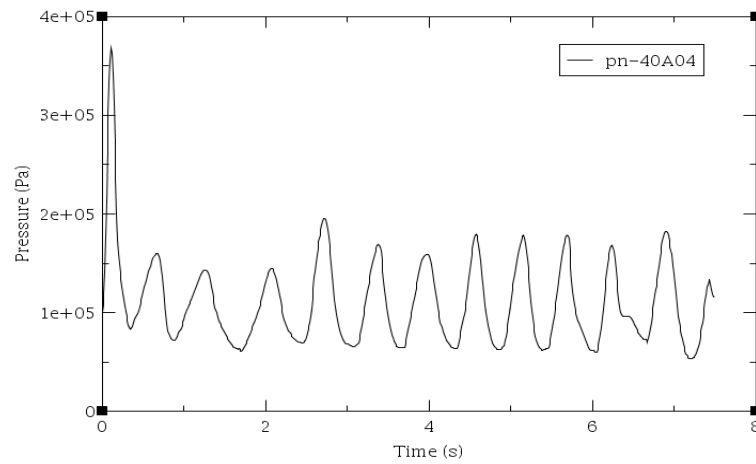


Figure 6-3: Water level oscillations in the hot side cylinder

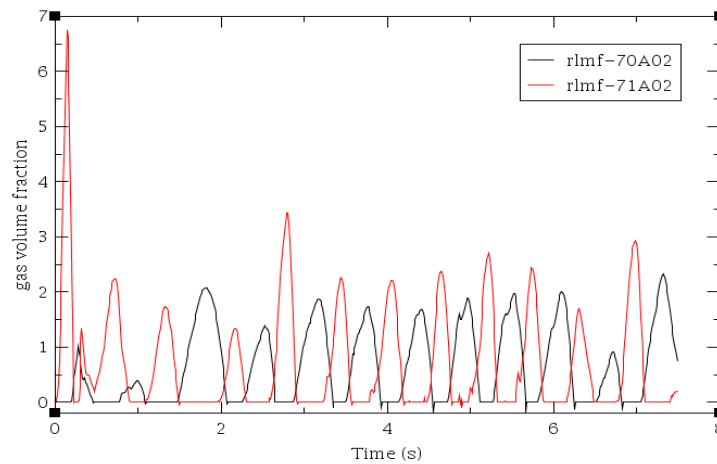


Figure 6-5: Mass flow through the top (red) and bottom (black) check valves

### Swarthmore Experimental Engine

Given the success of modeling West's engine, it is useful to have one more test to validate the modeling technique. The Swarthmore engine is an interesting choice to model because it was designed using the exact same design methodology that was used to design the engine in Chapter 3 of this paper. Similar to the results seen in our previous experiments in TRACE, the engine was able to see some oscillations, but could not deliver any useful pumping

through the check valves. So the success of this test will be indicated by the limited success of the engine. After learning that the engine did not provide pumping power, the Swarthmore team disconnected the pumping line to test again. The engine design with the pumping line attached can be seen in Figure 6-6 and its design specs are summarized in Table 6-1. The final design with the pumping line disconnected can be seen in Figure 6-7.

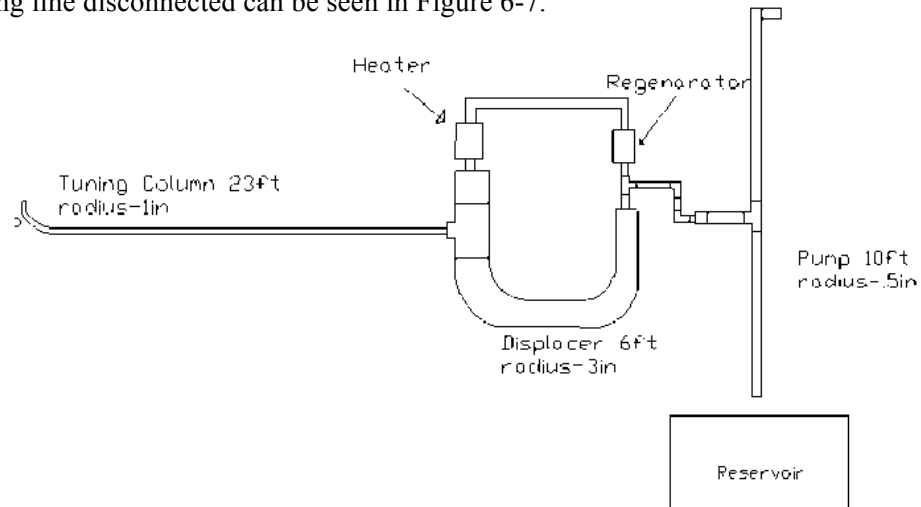


Figure 6-6: Swarthmore engine schematic with pumping line [11]

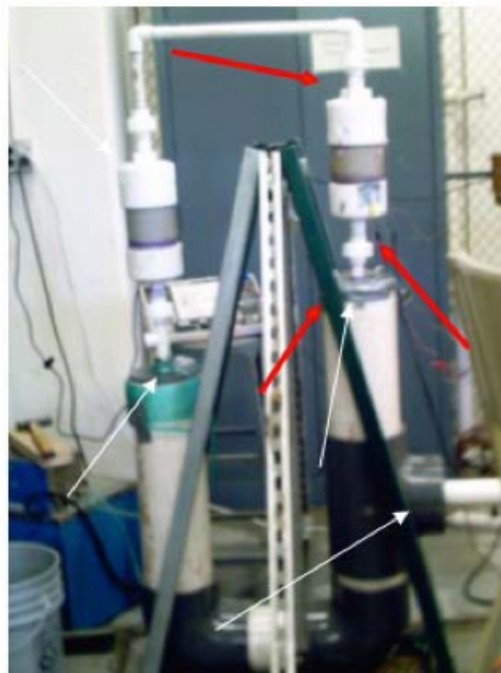


Figure 6-7: Swarthmore engine final design without pumping line [11]

Table 6-2: Swarthmore engine design specifications [11]

Parameter	Value
Working Fluid	Air
Material for displacer, tuning column, pump	Polyvinyl Chloride (PVC)
Support Frame	Unistrut
Insulating Float	Styrofoam
Oscillations Phase Angle	90°
Cold Cylinder Stroke	TBA
Cold Cylinder Diameter	6 inches (isothermalized)
Hot Cylinder Stroke	TBA
Hot cylinder diameter	6 inches (adiabatic)
Hot cylinder Float length	4 inches (above water level)
Float-cylinder gap	3.5mm
Tuning column diameter	50mm
Tuning column length (determined from equation 2.4.8)	23 feet
Pump-arm mean volume	133cm <sup>3</sup>
Regenerator internal volume	1440 cm <sup>3</sup>
Heater inner volume	1440 cm <sup>3</sup>
Dead space Volume	3250 cm <sup>3</sup>
Swept volume	7000 cm <sup>3</sup>
Heater Temperature	Max. 400 °C
Cold Temperature	10 °C

As a system of similar design was already modeled and explained in detail in Chapters 4 and 5, I will exclude such description here. The TRACE model for the Swarthmore engine is shown in Figure 6-8. The model was designed as closely as possible to the specifications in the Swarthmore design final report. Dimensions, volumes, materials, and connections were directly taken from the report. Because the engine was built with the same design guidelines as the engine in Chapter 4, only simple modifications had to be made to the earlier design to reflect the design detailed in Figure 6-6 and Table 6-1.

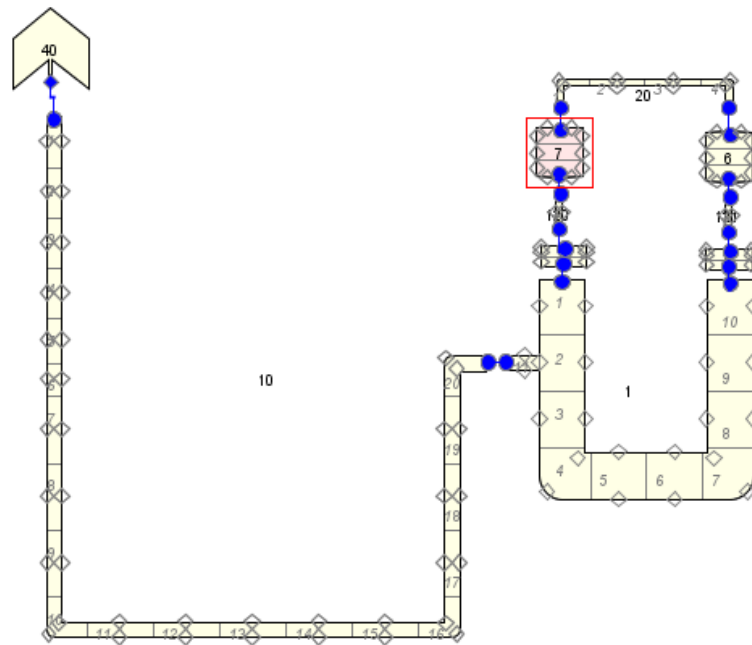


Figure 6-8: Model of Swarthmore engine final design [ ]

After designing the engine, a steady state calculation was run without heating to determine the initial conditions in the engine. The steady state calculation also confirms that the engine is built properly because the engine stays at rest. Applying a heat structure to the heater component and mimicking the regenerator design, a transient calculation was run to observe the engine behavior. Heating the heater and cooling the cold side cylinder starts oscillations in the system, as observed in previous testing. As was true with the physical engine, the model was marginally successful. Initial high levels of oscillation decayed overtime to small, continued oscillations. The Swarthmore report documents the temperature and pressure changes in the engine, as well as the tuning line output. In all of these areas, the model behaves similarly to the physical engine, with some limitations. Looking first at pressure changes in the engine, we can compare the Swarthmore engine results to the model results.

The Swarthmore engine's pressure oscillations were measured in the air connection tube between the heater and regenerator and can be seen in Figure 6-9. The engine started with



relatively high pressure oscillations before decaying at a 40s decay constant to steadier behavior with a mean pressure of around 102.5 kPa and amplitude of 2.5 kPa. As seen in Figure 6-10, the behavior of the model is similar. Initially high pressure amplitudes decay at a 35s decay constant to a mean pressure of around 102.5 kPa and amplitude of 2.5 kPa. This is a success for the model, as the pressure variations are accurately replicated. However, frequency in the model is higher than the physical engine and the model sustains high amplitude oscillation in the beginning for a longer period.

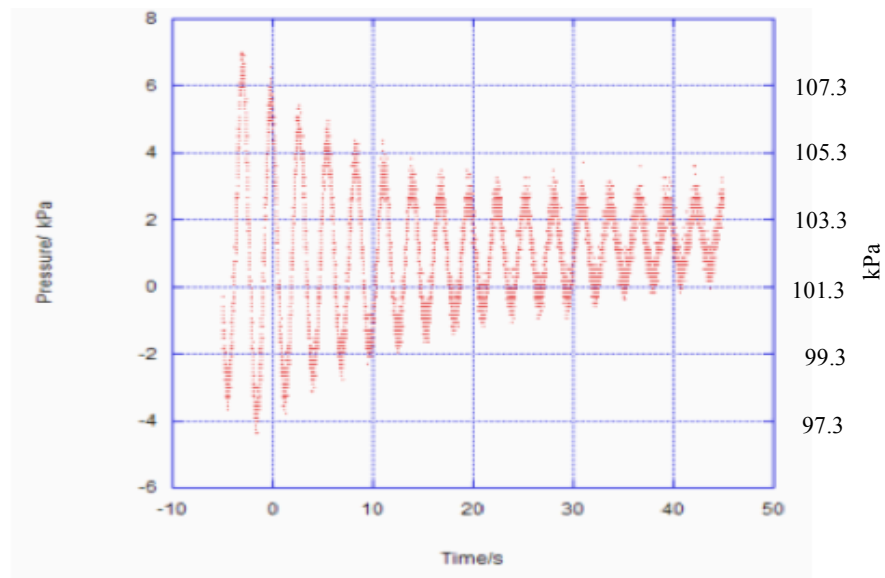


Figure 6-9: Pressure variations measured in Swarthmore engine [11]

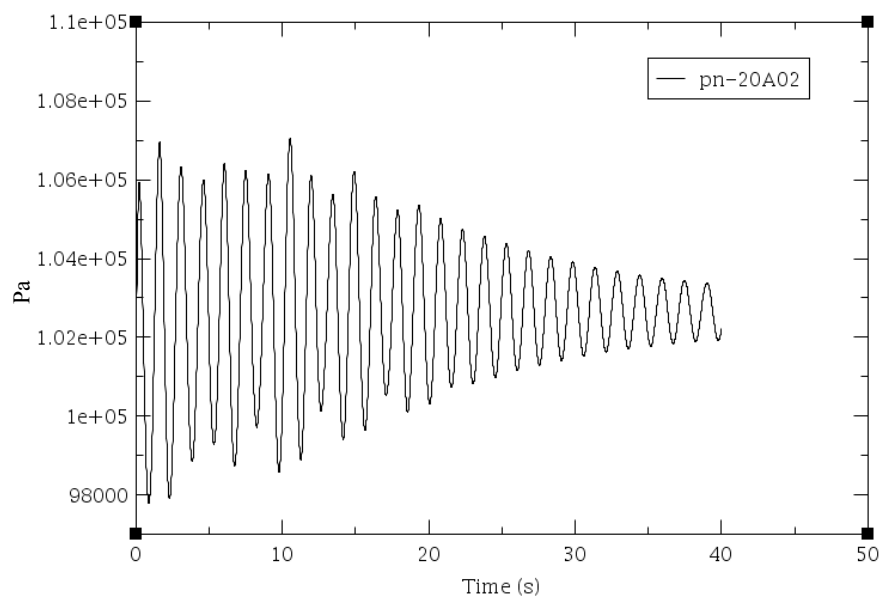


Figure 6-10: Pressure variations in model

The temperature variations in the model are also similar to the engine. The temperature variations in the heat exchanger of the Swarthmore engine can be seen in Figure 6-11. Here we see low frequency temperature variations between 175-350°C. Temperature variations in the heat exchanger of the model can be seen in Figure 6-12. Similarly, we see low frequency temperature variations, but temperatures are lower, varying between 125-175°C. The behavior similarity is a success and the temperature range difference is most likely due to the difficulty modeling the Swarthmore team's heating method.

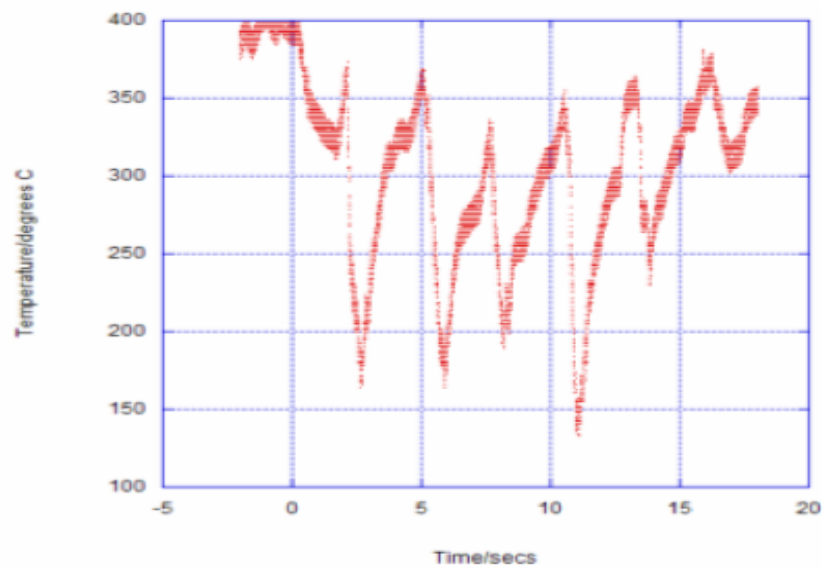


Figure 6-11: Temperature variations in Swarthmore heat exchanger [11]

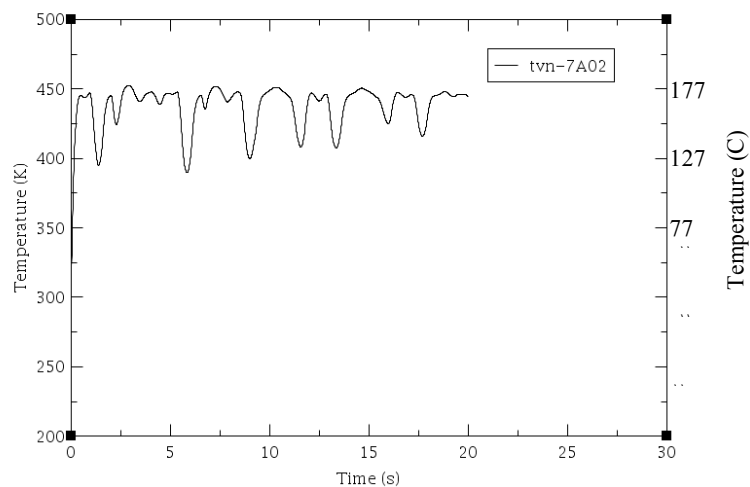


Figure 6-12: Temperature variations in model heat exchanger.

The Swarthmore team also measured the temperature variations in the hot side cylinder. These results can be seen in Figure 6-13. Temperature variations are once again low frequency and range between 25-37°C. Low temperatures like this in the hot cylinder can explain why oscillations are small and are most likely due to the small air connection between the hot side cylinder and the heater. Results in the model are similar once again. The results in Figure 6-14, show higher frequency variations, but in a similar temperature range of 29-42°C.

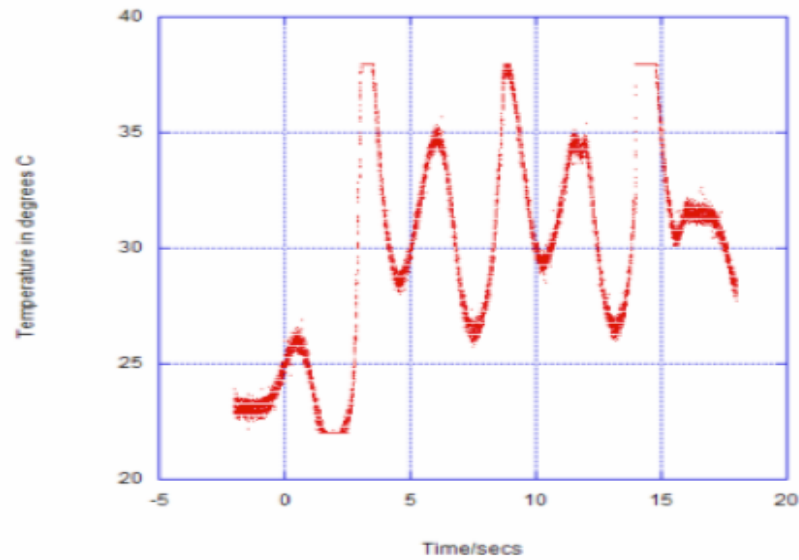


Figure 6-13: Temperature variations in Swarthmore hot cylinder [11].

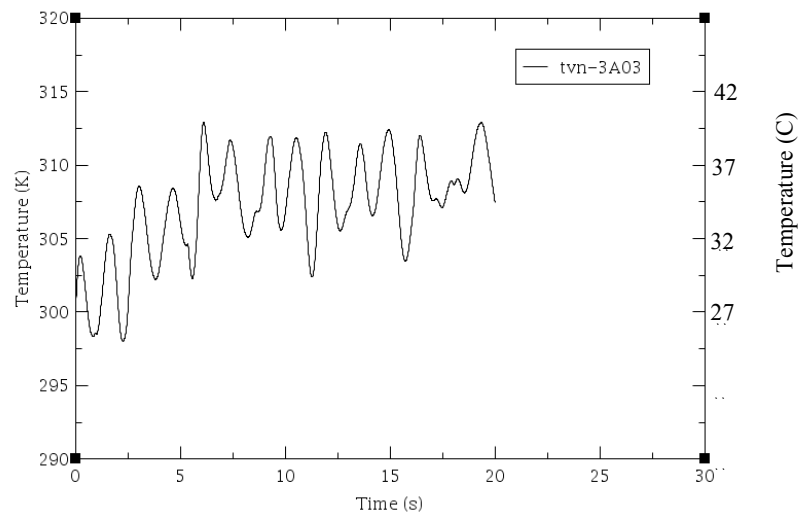


Figure 6-14: Temperature variations in model hot cylinder.

The final data provided by the Swarthmore team is the tuning line behavior. The team reported that the tuning line operated around 40Hz, with a velocity of around 0.6 m/s and amplitude of around 0.25m. The tuning line in the model behaved a bit differently than this. Velocity plots of the liquid in the tuning line indicate the model tuning line operated around 60Hz with a velocity around 0.9 m/s and amplitude of around 0.1m.

## **Chapter 7**

### **Results, Conclusions, and Recommendations**

The goal of this experimentation was to develop and validate a new computer modeling technique for liquid piston stirling engines. SNAP was chosen as graphical interface modeling platform that allows for quick and easy interactions with models both pre and post processing. With SNAP, models can be built easily in TRACE, a thermal-hydraulic, finite volume solver, that is excellent for two phase systems with complex flow and heat transfer relations. Starting with basic LPSE design guidelines and engine was designed and modeled piece by piece in SNAP/TRACE. The engine was broken down into smaller components that were easier to test to validate that their behavior is as expected. From there the entire engine was tested to observe behavior and analyze its operation. As this engine had never physically been built before, two additional engines documented by previous researchers were modeled and tested to determine whether they operate in the model as they did in physical testing.

### **Results**

Starting with the designed engine example resulted in mixed results. For one, it provided insight into the design relations and basic behavior of simple LPSE models. By going through the design process, assumptions for ideal operation and behavioral goals, such as displacer frequency, were explained so that the designs and basic tests were clearer. The individual tests that occurred in Chapter 4 showed the validity of modeling techniques of simple models, by observing non-complicated behavior. Free oscillation in the u-tube yielded an operational frequency very close to the natural frequency of the tube, as expected. Adding the tuning line design, both components operated at the same frequency with a 180 degree phase angle between tuning line and cold

cylinder. By oscillating air between a heating and cooling element, pressure oscillations were seen in the dead volume of the engine resulting in power output from a smaller u-tube. However, modeling a simple pump setup revealed difficulties with check valves in TRACE with added high frequency vibrations and potential errors in calculations.

Bringing all of the design together for the first time, the design proved a successful heat engine, but an unsuccessful water pump. Because the check valves causes problems, the first model tested did not include the pump setup. Starting from rest with heating components turned off, the system stayed at rest. Starting with a disturbance to cause oscillation without friction resulted in unending oscillations. By including friction in the model, oscillations died out with a reasonable decay constant. At this point, the model behaved as expected with all heating elements turned off. When heating elements turned on, the engine's success was evident as oscillations built up and were sustained over time. The design successful turned heat energy into mechanical energy, the definition of a heat engine. However, when the pump model was added into the system, the engine could not sustain oscillations because the pumping system absorbed too much energy for the displacer to continue its cycle.

The next design tested was a confirmed design built and tested by C.D. West and documented in his comprehensive book on LPSEs [1]. The engine was designed differently from the previous example. A tuning line was excluded, as was the regenerator and separate heating element. After modeling the engine as closely as possible to West's design and testing its basic behavior as done for the previous design, a 600K heat structure was applied to the hot side cylinder. After pressurization with local evaporation on the hot side, oscillations in the engine started when the top check valve opened allowing water to be pumped up and out of the engine, causing condensation and a pressure difference in the engine. Oscillations were successfully sustained over time with a large swing in pressure in the engine. The large pressure oscillations operated the pump setup as expected, pumping water out the top check valve and drawing water

in the bottom check valve in repetition. Overall the engine pumped about 500 L/hr to 1.6m head when provided a roughly 450W input (power can be measured from heat flux through the wall). This is similar to West's documented results of pumping 370 L/hr and 1.6 head provided a 540 W input.

Finally, an engine designed with the same design guidelines used in this paper was modeled and tested. Much like the first design modeled, this physical design technically functioned as a successful heat engine, but did not provide any useful pumping work through the check valves. While the engine designed in this paper has never been physically built and West's engine was documented limitedly, this engine was designed, built, and tested at Swarthmore and is well documented. The engine was modeled as closely as possible to the design detailed in the Swarthmore report and tested with similar conditions to the Swarthmore engine. Similar to the Swarthmore engine results, the model showed initial oscillations at high pressure that decayed to pressure oscillations at a similar mean pressure and amplitude. Similarly, temperature variations in the model are reasonably close to the physical engine. However, the engine did differ from the physical engine in tuning line behavior and operational frequency.

## **Conclusions**

The goal of the experimentation was successfully realized, as SNAP/TRACE was validated as a modeling technique for liquid piston stirling engines. Operation of simple engine components, like the displacer and heating components, was confirmed through a series of tests leading up to the testing of three LPSE designs. The first engine quickly confirmed the ability to show how a self-starting LPSE can convert heat energy into mechanical energy, but failed to produce useful pumping work. These results are entirely plausible, because the design has never been physically built and tested before. Despite the failure, the engine showed the successful

operation of heating and pipe components, and showed that the non-pumping portion of the engine functioned as expected.

Moving onto designs that had been physically built and tested, TRACE/SNAP was once again validated as a modeling technique because the models yielded similar results and behaviors to those of the physical engines. Modeling a simple engine/pump model designed by C.D. West yielded successful results as the engine self-started, maintained strong oscillations, and successfully pumped water through the check valve system. The pumping results were very similar to those documented by West, although West's documented results are somewhat unclear. Regardless, the engine functioned as expected and it was seen that a modeled engine could behave like its physical counterpart.

To confirm this, a second engine was tested that was designed and tested by a team at Swarthmore. The Swarthmore engine was designed around the same guidelines as the first engine designed and tested in this paper. Similarly to the engine from this paper, the Swarthmore engine proved to be a marginally successful heat engine, but an unsuccessful water pump. Creating and modeling to the same specifications as the Swarthmore team's final design, the model yielded results that agreed with the results documented by the Swarthmore team. Pressure and temperature behavior was very similar between the model and physical engine. Despite differences in tuning line behavior and frequency, the results were added confirmation that modeled engines could behave like their physical versions.

The results from these tests are significant. The modeling experiments confirmed that TRACE/SNAP can successfully model individual components and entire liquid piston stirling engines. It was confirmed that modeled engines can operate as heat engines and even show their ability to self-start and pump water. Finally, by modeling physical engines and comparing results between the model and engine, it was confirmed that the modeling technique can be used to predict and test the performance of liquid piston stirling engines.



The SNAP platform proved to be an incredibly easy and user-friendly interface to model engines. It provided a visual interface to see model layouts and modify designs, as well as pre-processing functionality to modify conditions and post-processing functionality to observe and plot results. TRACE proved to be a powerful thermal-hydraulic code that is fully capable of simulating the complex behaviors in liquid piston stirling engines. The capabilities of TRACE to handle two-phase flow, fluid dynamics, and heat transfer proved to be perfect for the liquid piston stirling engine models. With the confirmation of the modeling technique and the validity of TRACE/SNAP as a modeling platform for liquid piston stirling engines, we can confirm the hypothesis that TRACE/SNAP can be a modeling tool for liquid piston stirling engines. With this modeling technique, LPSE researchers and developers have a quick, easy, and cost-saving method for designing, testing, and developing liquid piston stirling engines.

### **Recommendations**

For the advancement of liquid piston stirling engine technologies, I have several suggestions and recommendations for future researchers. Here I will elaborate on general recommendations, excluding the many tips I have for modeling. The first of these suggestions have to do with making TRACE more accurate through a series of experiments that relate to fluid dynamics and heat transfer. This paper was kept relatively simple by excluding the discussion of several complicated fluid flow issues and making several assumptions, however, TRACE's capabilities greatly exceed those utilized in this experimentation. Therefore, I would suggest additional research into the following areas: using TRACE for two-phase flow, calibrating frictional losses for accurate friction factors, evaluating TRACE for oscillating flows, testing energy transfer in TRACE, and limiting TRACE errors.

If I had more time, I would have liked to explore more of TRACE's features and calculation capabilities. I used simple settings in TRACE and made several assumptions about how TRACE components would behave, but did not have the time to test all components individually. By running more testing and trying out more capabilities built into TRACE, models could be more accurate. Additionally, it would be interesting to build and test the engine designed in Chapters 4 and 5 of this paper. This would provide more insight into the validity of the modeling technique.

The shared marginal success of the Swarthmore engine and the engine designed in this paper draw some concerns regarding the design methodology used. One idea for the paper that I did not have the time to pursue was using the model to calculation design relations to create more accurate design guidelines. A future researcher could compare the design relations and equations used in the common LPSE design guidelines to the results when modeled in TRACE. I suggest that TRACE's computational abilities greatly exceed the mathematical relations used by these design guidelines that make many assumptions. TRACE could be used to improve the design guidelines commonly used.

I believe TRACE/SNAP has the capability to be a great tool for developing more efficient engines. Future researchers should test designs in TRACE/SNAP to predict their functionality and improve upon their designs. It would be quite easy and quick to observe how design changes affect functionality of engines. This could be a useful tool for optimization of engine designs.

Finally, as of the motivation of this paper was for the development of solar powered water pumping in developing countries. I suggest that future research efforts use TRACE/SNAP for the design, development, and improvement of solar powered LPSE water pumps. This modeling technique is a useful tool for testing models and should be used to aid the development of solar water pumps to provide water to those in communities in need of water supply.

## Appendix A

### Model Settings

Model Options - Properties View

Model Options

▼ General Show Disabled

Model Name	unnamed		
Title Cards	<none>	E	
Model Description	<none>	E	
Version	V 5.0 Patch 3		
Namelist Option	[1] INOPT Data After Title Cards		
Fluids	None	E	
Restart Number	<input type="checkbox"/>	Auto	
Start Time	<input type="checkbox"/>	Auto (s)	
Transient Calculation	[1] Transient		
Flow Parameter	[0] Liquid and Vapor Mass Flows		
Pressure Input Option	[0] Specify Pressures		
Water Packing	On		
Pressure Convergence	1.0E-4 (-)		
Steady-State Convergence	1.0E-4 (-)		
Pressure Iterations	10		
Steady-State Iterations	10		
Solute Tracking	[0] Off		
Namelist Variables	Valid values	E	
Namelist Variables	Valid values	E	
User Defined Units	< none >	E	
Timestep Data	[1] Timesteps	E	
Trip Initiated Timestep Data	[0] Timesteps	E	
System Gas/Liquids	None	E	
Noncond. Gas Option	<input checked="" type="checkbox"/> [1] Air		
Model Validation	[9] Active Tests: Loop Check, Noncondensable Partial Pressure Te...	E	
Initial Condition Sets	[0] Initial Condition Sets	E	
Sensitivity Coefficients	[38] coefficients available	E	

**Edit Timestep Data**

Initial Timestep Size:  s

End Time	Minimum Size	Maximum Size	Heat vs Fluid Size	Max Conv. Power Diff	Long Edit Interval	Graphics Interval	Restart Interval	Short Edit Interval
20.0	1.0E-6	0.01	10.0	1.0E20	10.0	0.01	100.0	1.0

**Edit Namelist Variables**

Filter:

☐ Show Disabled

▼ General			
Show Inactive Entries	<input checked="" type="radio"/> True <input type="radio"/> False		?
BLOCKAGEON - Blockage Flow Loss	<input type="checkbox"/> True <input checked="" type="radio"/> False		?
CCIF - Const 2P Drag	<input type="checkbox"/> <input type="text" value="1.0E4"/> (kg/m <sup>4</sup> )	◀▶	?
CHFMULT - CHF Multiplier	<input type="checkbox"/> <input type="text" value="1.0"/> (-)	◀▶	?
CLOSEST - Closest Timestep	<input type="checkbox"/> True <input checked="" type="radio"/> False		?
CPUFLAG - CPU Time Flag	<input type="checkbox"/> <input type="text" value="&lt; Inactive &gt;"/>	▼	?
CSSMAXNUMOPT - CSS Max Number	<input type="checkbox"/> True <input checked="" type="radio"/> False		?
DOXLAYER - Default Oxide Layer	<input type="checkbox"/> <input type="text" value="0.0"/> (m)	◀▶	?
DTSTRT - Initial timestep size	<input checked="" type="checkbox"/> <input type="text" value="-1.0"/> (s)	◀▶	?
ECRPLIMIT - ECRP Limit	<input type="checkbox"/> <input type="text" value="17.0"/> (-)	◀▶	?
FDHFL	<input type="checkbox"/> <input type="text" value="1.0"/> (-)	◀▶	?
FORCEBU - Force Time Backup	<input type="checkbox"/> <input type="text" value="Unknown"/> (s)	◀▶	?
FLOWDEPK - Flow Dependent Losses	<input type="checkbox"/> True <input checked="" type="radio"/> False		?
FOXlayer - Fuel Oxide Layer	<input type="checkbox"/> <input type="text" value="&lt; Inactive &gt;"/>	▼	?
FPMAX - Max Power Change	<input type="checkbox"/> <input type="text" value="0.1"/> (-)	◀▶	?
FPOWERDE - Max Power Decrease	<input type="checkbox"/> <input type="text" value="0.1"/> (-)	◀▶	?
FPOWERIN - Max Power Increase	<input type="checkbox"/> <input type="text" value="0.02"/> (-)	◀▶	?
FREACTDE - Max Reactivity Decrease	<input type="checkbox"/> <input type="text" value="0.05"/> (-)	◀▶	?
FREACTIN - Max Reactivity Increase	<input type="checkbox"/> <input type="text" value="0.01"/> (-)	◀▶	?
HOMMULTAWD - Homogenous Mult.	<input type="checkbox"/> True <input checked="" type="radio"/> False		?
HTCWL - Const wall-liquid HTC	<input type="checkbox"/> <input type="text" value="10.0"/> (W/m <sup>2</sup> /K)	◀▶	?

HTCWL - Const wall-liquid HTC	<input type="checkbox"/>	10.0 (W/m <sup>2</sup> /K)	◀▶	?
HTCWV - Const wall-vapor HTC	<input type="checkbox"/>	10.0 (W/m <sup>2</sup> /K)	◀▶	?
IAMABWR - BWR Vessel Option	<input type="checkbox"/>	<input type="radio"/> True <input checked="" type="radio"/> False		?
IBLAUS - Blasius Drag Option	<input type="checkbox"/>	< Inactive >	▼	?
ICDELT - Initial DELT Option	<input type="checkbox"/>	< Inactive >	▼	?
ICONHT - Heat-transfer option	<input type="checkbox"/>	< Inactive >	▼	?
IELV - Elevation Option	<input type="checkbox"/>	< Inactive >	▼	?
IFLCOND - Fluid Conduction Flag	<input type="checkbox"/>	< Inactive >	▼	?
IGEOM3 - Vessel Area Option	<input type="checkbox"/>	< Inactive >	▼	?
IH2SRC - H2 Source Flag	<input type="checkbox"/>			?
IHOR - Wall-drag Option	<input checked="" type="checkbox"/>	[1] Dispersed/Stratified	▼	?
IKFAC - Friction Option	<input checked="" type="checkbox"/>	[1] K-Factors	▼	?
IMPWALLHT - Implicit Wall Heat	<input type="checkbox"/>	< Inactive >	▼	?
INVAN - Inverted Annular Switch	<input type="checkbox"/>	< Inactive >	▼	?
IOFFTK - TEE Offtake Model	<input type="checkbox"/>	< Inactive >	▼	?
IOINP - Input File Units	<input type="checkbox"/>	< Inactive >	▼	?
IPOWR - Power Initialization	<input type="checkbox"/>	< Inactive >	▼	?
IRESET - Reset Energy	<input type="checkbox"/>	< Inactive >	▼	?
ISOLCN - Solubility-parameters	<input type="checkbox"/>	< Inactive >	▼	?

ISOLCN - Solubility-parameters	<input type="checkbox"/>	< Inactive >	?
ISOLVEDEF - Default Heat Conduction	<input type="checkbox"/>	< Inactive >	?
ISSCVT - SS Convergence Test	<input type="checkbox"/>	< Inactive >	?
ITDMR - Coupled Neutronics	<input type="checkbox"/>	< Inactive >	?
ITHD - HD from HDRI/O	<input type="checkbox"/>	< Inactive >	?
LBDRAG - Vessel Drag Option	<input type="checkbox"/>	<input type="radio"/> True <input checked="" type="radio"/> False	?
IWRITEMSG LIM - Output Warning Limit	<input type="checkbox"/>		?
MULTBFL - Blockage Loss Multiplier	<input type="checkbox"/>	1.0 (-) <>	?
NCONTANT - Containment Calculation	<input type="checkbox"/>	< Inactive >	?
NDIA1 - Input Heated Diameters	<input type="checkbox"/>	< Inactive >	?
NFRC1 - Input 1D Rev FRIC	<input type="checkbox"/>	< Inactive >	?
NFRC3 - Input 3D Rev FRIC	<input type="checkbox"/>	< Inactive >	?
NIFSH - Shear Option	<input type="checkbox"/>	< Inactive >	?
NLT - Num Loops	<input type="checkbox"/>		?
NOAIR - NC Pressure Calc	<input checked="" type="checkbox"/>	[0] NC Calc On	?
NOFAT - No Flow Area Test	<input checked="" type="checkbox"/>	<input checked="" type="radio"/> True <input type="radio"/> False	?
NOLT1D - 1D Level Tracking	<input type="checkbox"/>	< Inactive >	?
NOLT3D - 3D Level Tracking	<input type="checkbox"/>	< Inactive >	?
NOSETS - SETS Numerics	<input type="checkbox"/>	< Inactive >	?

NOSETS - SETS Numerics	<input type="checkbox"/>	< Inactive >	?
NRSLV - Axial Conduction	<input type="checkbox"/>	< Inactive >	?
NSEND - End Timestep	<input type="checkbox"/>		?
NSOLVER - SuperLU Solver	<input type="checkbox"/>	< Inactive >	?
NVGRAV - 3d Gravity Vector	<input type="checkbox"/>	< Inactive >	?
PUMPFRIQ - Pump Impeller Option	<input type="checkbox"/>	<input type="radio"/> True <input checked="" type="radio"/> False	?
TDMRRAMP - Power Ramp	<input type="checkbox"/>		?
TPOWR - Time SS Power On	<input type="checkbox"/>	1.0E30 (s) <input type="button" value="Left"/> <input type="button" value="Right"/>	?
USE_D2O_ST - Heavy Water Flag	<input type="checkbox"/>	<input type="radio"/> True <input checked="" type="radio"/> False	?
USE_IAPWS_ST - Steam table flag	<input type="checkbox"/>	<input type="radio"/> True <input checked="" type="radio"/> False	?
USESJC - Use Single Jun Components		[3] SJs with Angle Input	?
USE_MODNFI_K - Use Modified NFI Correlation	<input type="checkbox"/>	<input type="radio"/> True <input checked="" type="radio"/> False	?
VIEWFACTREVERSE - TRAC-B View Factors	<input type="checkbox"/>	<input type="radio"/> True <input checked="" type="radio"/> False	?
▶ Default Initial Conditions			
▶ Choke Flow Options			
▶ Output Options			
▶ Diagnostics			
▼ Design Factors			
MHTLI - Inner Liquid	<input type="checkbox"/>	< Inactive >	?
MHTLO - Outer Liquid	<input type="checkbox"/>	< Inactive >	?
MHTVI - Inner Vapor	<input type="checkbox"/>	< Inactive >	?
MHTVO - Outer Vapor	<input type="checkbox"/>	< Inactive >	?
MWFL - Liquid Wall Friction	<input checked="" type="checkbox"/>	[1] Yes	?
MWFV - Vapor Wall Friction	<input checked="" type="checkbox"/>	[1] Yes	?
▶ RELAP5 Options			

Pipe 6 (Regenerator) - Properties View

Pipe 6 (Regenerator)  
Hydro Connections

▼ General Show Disabled

Component Name	Regenerator	
Component Number		6
Description	<none>	
Component Geometry	Cells: 5	
Initial Conditions	[ Valid Conditions ]	
Friction	Kfac ( 0.0, 0.0, 0.0, 0.0, 0.0, 0.0 )	
Fluid Power Options	Not Modeled	
Wall Roughness		0.0 (m)
Inlet	Pipe 121 Cell 1 outlet	
Outlet	Pipe 20 Cell 4 outlet	
Cross Flow Connections	[0] Connections	
Pipe Type	[0] No Accumulator	
Number of Pipes		1
Leak Paths	[0] Leak Paths	

▼ Pipe Wall

Use Pipewall	<input checked="" type="radio"/> True <input type="radio"/> False	
Critical Heat Flux	[1] AECL_IPPE	
Variable Radial Mesh	<input type="radio"/> True <input checked="" type="radio"/> False	
Radial Nodes		2
Pipewall Material	Material 6 (Stainless 304)	
Wall Temperature	[5][2] Temperature Values	
Outside Component	Constant BCs	
Inner Radius		0.0635 (m)
Wall Thickness		0.02 (m)
Liquid Heat Transfer		0.0 (W/m <sup>2</sup> /K)
Vapor Heat Transfer		0.0 (W/m <sup>2</sup> /K)
Outside Liquid Temp.		300.0 (K)
Outside Vapor Temp.		300.0 (K)

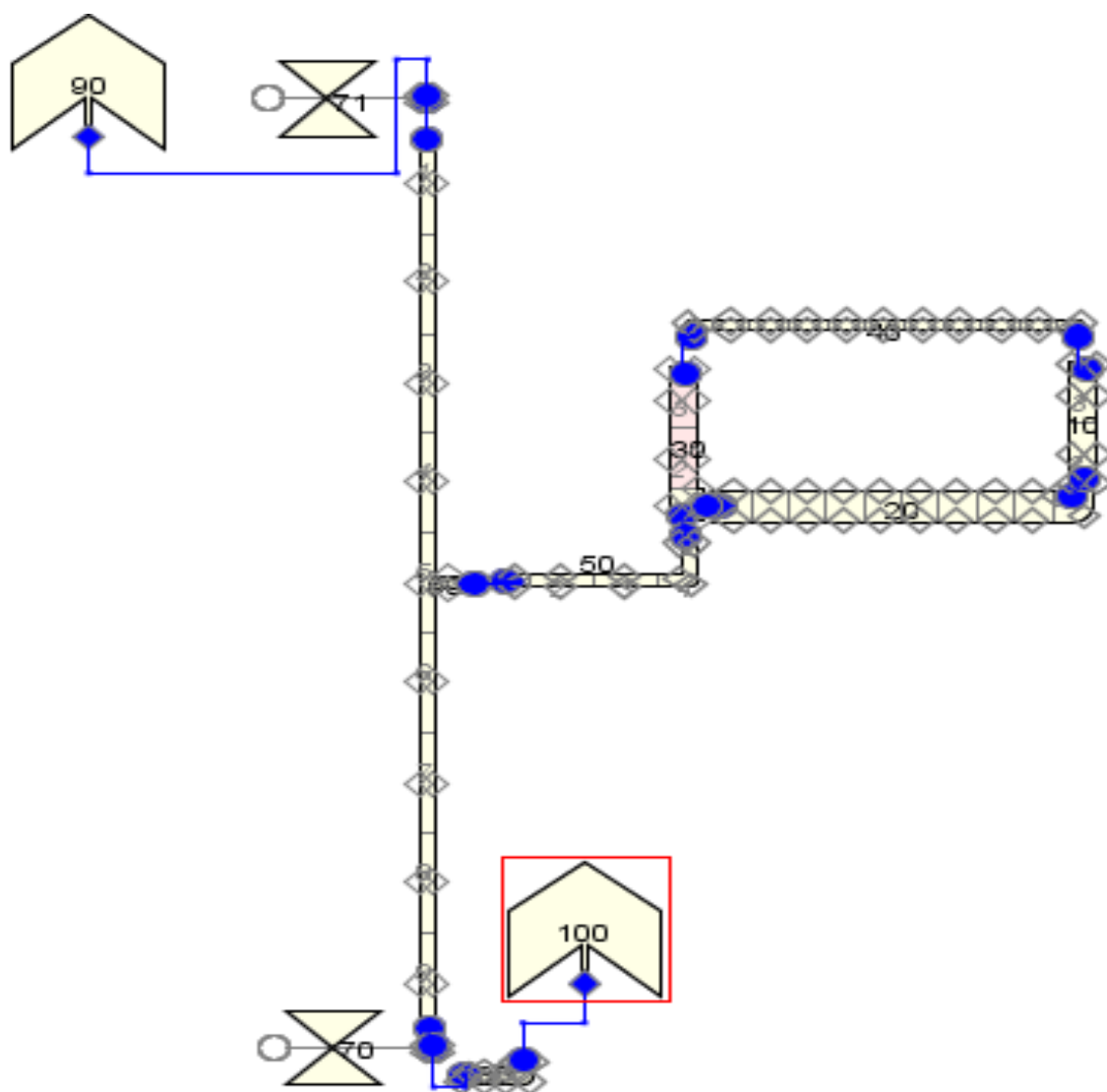
► Wall Power

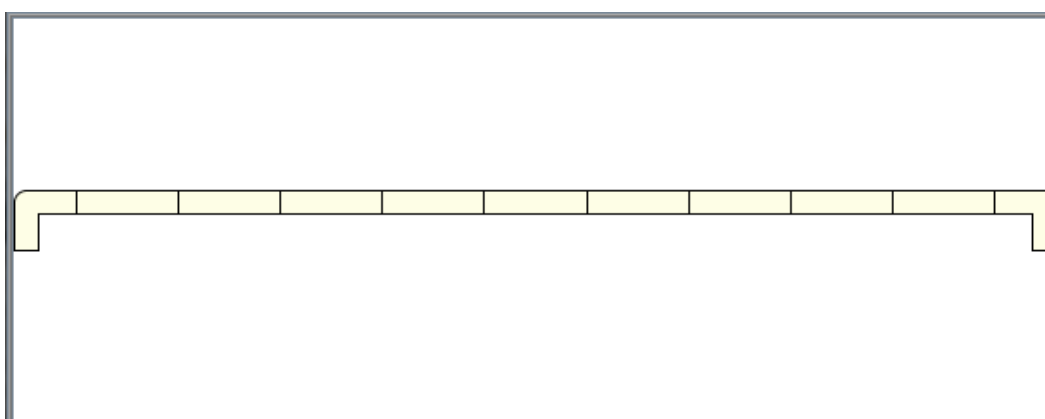
► Trace Species



## Appendix B

## West Engine Model Geometry
















Cell Number	Volume (m³)	Length (m)	Vol. Avg. Flow Area (m²)	DZ (m)	2D Drawing Pivot
1	1.884E-5	0.06	3.14E-4	0.03	<input type="checkbox"/>
2	1.884E-5	0.06	3.14E-4	0.0	<input type="checkbox"/>
3	1.884E-5	0.06	3.14E-4	0.0	<input type="checkbox"/>
4	1.884E-5	0.06	3.14E-4	0.0	<input type="checkbox"/>
5	1.884E-5	0.06	3.14E-4	0.0	<input type="checkbox"/>
6	1.884E-5	0.06	3.14E-4	0.0	<input type="checkbox"/>
7	1.884E-5	0.06	3.14E-4	0.0	<input type="checkbox"/>
8	1.884E-5	0.06	3.14E-4	0.0	<input type="checkbox"/>
9	1.884E-5	0.06	3.14E-4	0.0	<input type="checkbox"/>
10	1.884E-5	0.06	3.14E-4	0.0	<input type="checkbox"/>
11	1.884E-5	0.06	3.14E-4	-0.03	<input type="checkbox"/>
Total	2.0724E-4	0.66	3.454E-3	0.0	

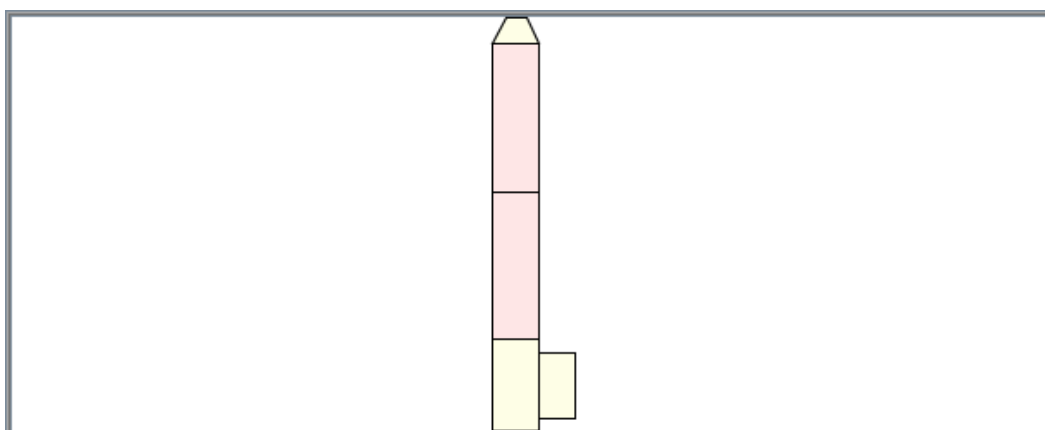
Edge Number	Flow Area (m²)	Calculate Hydraulic Diam.	Hydraulic Diam. (m)	CCFL Model
1	3.14E-4	<input type="checkbox"/>	0.02	<none>
2	3.14E-4	<input type="checkbox"/>	0.02	<none>
3	3.14E-4	<input type="checkbox"/>	0.02	<none>
4	3.14E-4	<input type="checkbox"/>	0.02	<none>
5	3.14E-4	<input type="checkbox"/>	0.02	<none>
6	3.14E-4	<input type="checkbox"/>	0.02	<none>
7	3.14E-4	<input type="checkbox"/>	0.02	<none>
8	3.14E-4	<input type="checkbox"/>	0.02	<none>
9	3.14E-4	<input type="checkbox"/>	0.02	<none>
10	3.14E-4	<input type="checkbox"/>	0.02	<none>
11	3.14E-4	<input type="checkbox"/>	0.02	<none>
12	3.14E-4	<input type="checkbox"/>	0.02	<none>

Edge Number	Orientation	Angle $\Theta$ (rad)	Grav sin( $\Theta$ )	Cell DZ (m)
1		1.571	1.0	0.03
2		0.0	0.0	0.0
3		0.0	0.0	0.0
4		0.0	0.0	0.0
5		0.0	0.0	0.0
6		0.0	0.0	0.0
7		0.0	0.0	0.0
8		0.0	0.0	0.0
9		0.0	0.0	0.0
10		0.0	0.0	0.0
11		0.0	0.0	-0.03
12		-1.571	-1.0	


Cell Number	Volume (m <sup>3</sup> )	Length (m)	Vol. Avg. Flow Area (m <sup>2</sup> )	DZ (m)	2D Drawing Pivot
1	1.852649E-4	0.0585	3.166922E-3	0.0	<input type="checkbox"/>
2	1.852649E-4	0.0585	3.166922E-3	0.0	<input type="checkbox"/>
3	1.852649E-4	0.0585	3.166922E-3	0.0	<input type="checkbox"/>
4	1.852649E-4	0.0585	3.166922E-3	0.0	<input type="checkbox"/>
5	1.852649E-4	0.0585	3.166922E-3	0.0	<input type="checkbox"/>
6	1.852649E-4	0.0585	3.166922E-3	0.0	<input type="checkbox"/>
7	1.852649E-4	0.0585	3.166922E-3	0.0	<input type="checkbox"/>
8	1.852649E-4	0.0585	3.166922E-3	0.0	<input type="checkbox"/>
9	1.852649E-4	0.0585	3.166922E-3	0.0	<input type="checkbox"/>
10	2.010995E-4	0.0635	3.166922E-3	0.03175	<input type="checkbox"/>
Total	1.868484E-3	0.59	0.031669217	0.03175	

Edge Number	Flow Area (m <sup>2</sup> )	Calculate Hydraulic Diam.	Hydraulic Diam. (m)	CCFL Model
1	3.166922E-3	<input type="checkbox"/>	0.0635	<none>
2	3.166922E-3	<input type="checkbox"/>	0.0635	<none>
3	3.166922E-3	<input type="checkbox"/>	0.0635	<none>
4	3.166922E-3	<input type="checkbox"/>	0.0635	<none>
5	3.166922E-3	<input type="checkbox"/>	0.0635	<none>
6	3.166922E-3	<input type="checkbox"/>	0.0635	<none>
7	3.166922E-3	<input type="checkbox"/>	0.0635	<none>
8	3.166922E-3	<input type="checkbox"/>	0.0635	<none>
9	3.166922E-3	<input type="checkbox"/>	0.0635	<none>
10	3.166922E-3	<input type="checkbox"/>	0.0635	<none>
11	3.166922E-3	<input type="checkbox"/>	0.0635	<none>

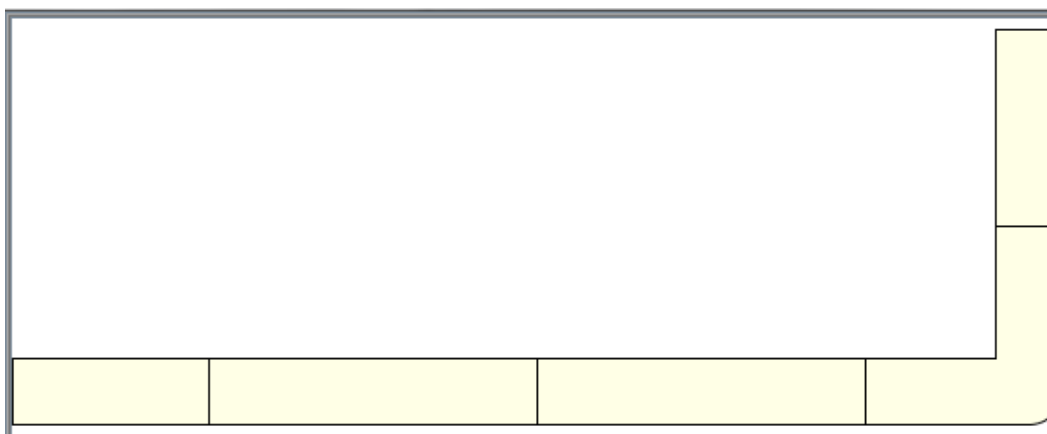
Edge Number	Orientation	Angle $\Theta$ (rad)	Grav sin( $\Theta$ )	Cell DZ (m)
1		0.0	0.0	0.0
2		0.0	0.0	0.0
3		0.0	0.0	0.0
4		0.0	0.0	0.0
5		0.0	0.0	0.0
6		0.0	0.0	0.0
7		0.0	0.0	0.0
8		0.0	0.0	0.0
9		0.0	0.0	0.0
10		0.0	0.0	0.03175
11		1.571	1.0	



Cell Number	Volume (m³)	Length (m)	Vol. Avg. Flow Area (m²)	DZ (m)	2D Drawing Pivot
1	1.000906E-4	0.0645	1.551792E-3	0.0645	<input type="checkbox"/>
2	1.833054E-4	0.118125	1.551792E-3	0.118125	<input type="checkbox"/>
3	1.833054E-4	0.118125	1.551792E-3	0.118125	<input type="checkbox"/>
4	1.551792E-6	1.0E-3	1.551792E-3	1.0E-3	<input type="checkbox"/>
5	3.166922E-5	0.01	3.166922E-3	0.0	<input type="checkbox"/>
Total	4.999225E-4	0.31175	9.37409E-3	0.30175 / 0.032...	

Edge Number	Flow Area (m²)	Calculate Hydraulic Diam.	Hydraulic Diam. (m)	CCFL Model
1	1.551792E-3	<input type="checkbox"/>	0.04445	<none>
2	1.551792E-3	<input type="checkbox"/>	0.04445	<none>
3	1.551792E-3	<input type="checkbox"/>	0.04445	<none>
4	1.551792E-3	<input type="checkbox"/>	0.04445	<none>
5	3.14E-4	<input type="checkbox"/>	0.02	<none>
6	3.166922E-3	<input type="checkbox"/>	0.0635	<none>
7	3.166922E-3	<input type="checkbox"/>	0.0635	<none>

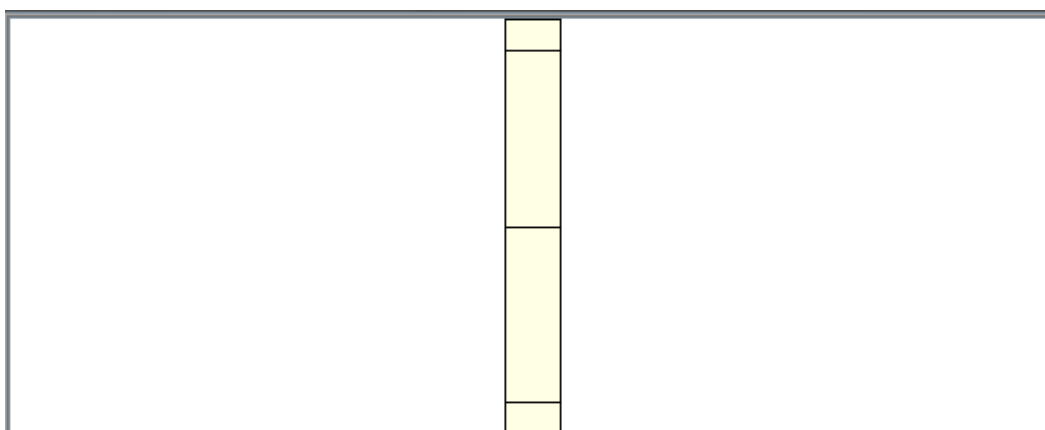
Edge Number	Orientation	Angle $\Theta$ (rad)	Grav sin( $\Theta$ )	Cell DZ (m)
1		1.571	1.0	0.0645
2		1.571	1.0	0.118125
3		1.571	1.0	0.118125
4		1.571	1.0	1.0E-3
5		1.571	1.0	
6		0.0	0.0	0.0
7		0.0	0.0	



Cell Number	Volume (m³)	Length (m)	Vol. Avg. Flow Area (m²)	DZ (m)	2D Drawing Pivot
1	2.533537E-5	0.05	5.067075E-4	0.0	<input type="checkbox"/>
2	5.067075E-5	0.1	5.067075E-4	0.0	<input type="checkbox"/>
3	5.067075E-5	0.1	5.067075E-4	0.0	<input type="checkbox"/>
4	5.067075E-5	0.1	5.067075E-4	0.05	<input type="checkbox"/>
5	2.533537E-5	0.05	5.067075E-4	0.05	<input type="checkbox"/>
Total	2.02683E-4	0.4	2.533537E-3	0.1	

Edge Number	Flow Area (m²)	Calculate Hydraulic Diam.	Hydraulic Diam. (m)	CCFL Model
1	5.07E-4	<input type="checkbox"/>	0.025407331	<none>
2	5.067075E-4	<input type="checkbox"/>	0.0254	<none>
3	5.067075E-4	<input type="checkbox"/>	0.0254	<none>
4	5.067075E-4	<input type="checkbox"/>	0.0254	<none>
5	5.067075E-4	<input type="checkbox"/>	0.0254	<none>
6	1.551792E-3	<input type="checkbox"/>	0.04445	<none>

Edge Number	Orientation	Angle $\Theta$ (rad)	Grav sin( $\Theta$ )	Cell DZ (m)
1		0.0	0.0	0.0
2		0.0	0.0	0.0
3		0.0	0.0	0.0
4		0.0	0.0	0.05
5		1.571	1.0	0.05
6		1.571	1.0	



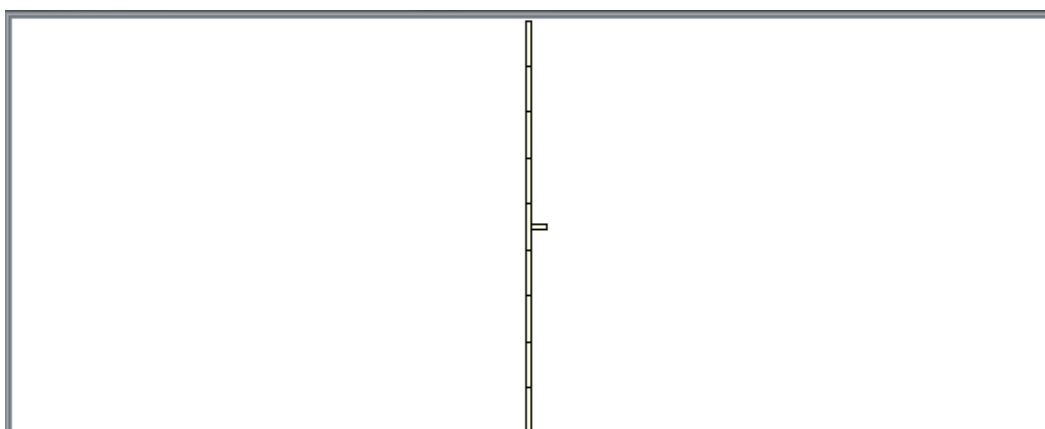
Cell Number	Volume (m³)	Length (m)	Vol. Avg. Flow Area (m²)	DZ (m)	2D Drawing Pivot
1	1.551792E-6	1.0E-3	1.551792E-3	1.0E-3	<input type="checkbox"/>
2	1.833054E-4	0.118125	1.551792E-3	0.118125	<input type="checkbox"/>
3	1.833054E-4	0.118125	1.551792E-3	0.118125	<input type="checkbox"/>
4	1.551792E-6	1.0E-3	1.551792E-3	1.0E-3	<input type="checkbox"/>
Total	3.697144E-4	0.23825	6.207167E-3	0.23825	

Edge Number	Flow Area (m²)	Calculate Hydraulic Diam.	Hydraulic Diam. (m)	CCFL Model
1	3.166922E-3	<input type="checkbox"/>	0.0635	<none>
2	1.551792E-3	<input type="checkbox"/>	0.04445	<none>
3	1.551792E-3	<input type="checkbox"/>	0.04445	<none>
4	1.551792E-3	<input type="checkbox"/>	0.04445	<none>
5	3.14E-4	<input type="checkbox"/>	0.02	<none>








Edge Number	Orientation	Angle $\theta$ (rad)	Grav sin( $\theta$ )	Cell DZ (m)
1		1.571	1.0	1.0E-3
2		1.571	1.0	0.118125
3		1.571	1.0	0.118125
4		1.571	1.0	1.0E-3
5		1.571	1.0	



Cell Number	Volume (m <sup>3</sup> )	Length (m)	Vol. Avg. Flow Area (m <sup>2</sup> )	DZ (m)	2D Drawing Pivot
1	1.014E-4	0.2	5.07E-4	-0.2	<input type="checkbox"/>
2	1.014E-4	0.2	5.07E-4	-0.2	<input type="checkbox"/>
3	1.014E-4	0.2	5.07E-4	-0.2	<input type="checkbox"/>
4	1.014E-4	0.2	5.07E-4	-0.2	<input type="checkbox"/>
5	1.014E-4	0.2	5.07E-4	-0.2	<input type="checkbox"/>
6	1.014E-4	0.2	5.07E-4	-0.2	<input type="checkbox"/>
7	1.014E-4	0.2	5.07E-4	-0.2	<input type="checkbox"/>
8	1.014E-4	0.2	5.07E-4	-0.2	<input type="checkbox"/>
9	1.014E-4	0.2	5.07E-4	-0.2	<input type="checkbox"/>
10	2.535E-5	0.05	5.07E-4	0.0	<input type="checkbox"/>
<b>Total</b>	<b>9.3795E-4</b>	<b>1.85</b>	<b>5.07E-3</b>	<b>-1.8 / -0.9</b>	

Edge Number	Flow Area (m <sup>2</sup> )	Calculate Hydraulic Diam.	Hydraulic Diam. (m)	CCFL Model
1	5.07E-4	<input type="checkbox"/>	0.025407331	<none>
2	5.07E-4	<input type="checkbox"/>	0.025407331	<none>
3	5.07E-4	<input type="checkbox"/>	0.025407331	<none>
4	5.07E-4	<input type="checkbox"/>	0.025407331	<none>
5	5.07E-4	<input type="checkbox"/>	0.025407331	<none>
6	5.07E-4	<input type="checkbox"/>	0.025407331	<none>
7	5.07E-4	<input type="checkbox"/>	0.025407331	<none>
8	5.07E-4	<input type="checkbox"/>	0.025407331	<none>
9	5.07E-4	<input type="checkbox"/>	0.025407331	<none>
10	5.067075E-4	<input type="checkbox"/>	0.0254	<none>
11	5.07E-4	<input type="checkbox"/>	0.025407331	<none>
12	5.07E-4	<input type="checkbox"/>	0.025407331	<none>

Edge Number	Orientation	Angle $\Theta$ (rad)	Grav sin( $\Theta$ )	Cell DZ (m)
1		-1.571	-1.0	-0.2
2		-1.571	-1.0	-0.2
3		-1.571	-1.0	-0.2
4		-1.571	-1.0	-0.2
5		-1.571	-1.0	-0.2
6		-1.571	-1.0	-0.2
7		-1.571	-1.0	-0.2
8		-1.571	-1.0	-0.2
9		-1.571	-1.0	-0.2
10		-1.571	-1.0	-0.2
11		0.0	0.0	0.0
12		0.0	0.0	0.0

					
Cell Number	Volume (m³)	Length (m)	Vol. Avg. Flow Area (m²)	DZ (m)	2D Drawing Pivot
1	1.520122E-5	0.03	5.067075E-4	-0.015	<input type="checkbox"/>
2	1.520122E-5	0.03	5.067075E-4	0.0	<input type="checkbox"/>
3	1.520122E-5	0.03	5.067075E-4	0.0	<input type="checkbox"/>
4	1.520122E-5	0.03	5.067075E-4	0.015	<input type="checkbox"/>
5	1.520122E-5	0.03	5.067075E-4	0.03	<input type="checkbox"/>
Total	7.600612E-5	0.15	2.533537E-3	0.03	
Edge Number	Flow Area (m²)	Calculate Hydraulic Diam.	Hydraulic Diam. (m)	CCFL Model	
1	5.067075E-4	<input type="checkbox"/>	0.0254	<none>	
2	5.067075E-4	<input type="checkbox"/>	0.0254	<none>	
3	5.067075E-4	<input type="checkbox"/>	0.0254	<none>	
4	5.067075E-4	<input type="checkbox"/>	0.0254	<none>	
5	5.067075E-4	<input type="checkbox"/>	0.0254	<none>	
6	5.067075E-4	<input type="checkbox"/>	0.0254	<none>	
Edge Number	Orientation	Angle $\Theta$ (rad)	Grav sin( $\Theta$ )	Cell DZ (m)	
1		-1.571	-1.0	-0.015	
2		0.0	0.0	0.0	
3		0.0	0.0	0.0	
4		0.0	0.0	0.015	
5		1.571	1.0	0.03	
6		1.571	1.0		



Heat Structure 130

- Supplemental Rods [0]
- Heatstructure Connections

▼ General ☐ Show Disabled

Component Name	unnamed	
Component Number	130	
Description	<none>	
Axial Nodes / Surface BCs	2 Axial Cells	
Critical Heat Flux	[1] AECL_IPPE	
Fuel Rod Option	[1] Not Fuel Rod	

Surfaces - Heat Structure 130

Inner Surface Boundary Conditions	Axial Cell	Outer Surface Boundary Conditions
[2] Tee: 30 Cell: 2	1	[5] Surf Temp: 600.0
[2] Tee: 30 Cell: 3	2	[5] Surf Temp: 600.0

Split Merge Add Remove

▼ General ☐ Show Disabled

No Properties Available

OK Cancel

Maximum Axial Nodes 100

Break 90  
Hydro Connections




General		Show Disabled
Component Name	unnamed	
Component Number	90	
Break Type	[0] No Tables	
Temperature Table Option	[0] Enter liquid/gas temp	
Fluid State Option	[0] Last Interp State Held Const.	
Description	<none>	
Inlet	Valve 71 Cell 2 outlet	
Length	0.0127 (m)	
Volume	6.435185E-6 (m³)	
Initial Gas Volume Fraction	1.0 (-)	
Initial Mixture Temperature	300.0 (K)	
Initial Pressure	1.01352E5 (Pa)	
Initial Noncondensable PP	1.01352E5 (Pa)	
Adjacent Pressure Flag	<input type="radio"/> True <input checked="" type="radio"/> False	
Max Pressure Change Rate	1.0E20 (Pa/s)	














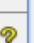

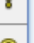

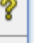

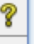

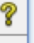

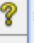

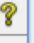

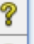

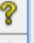

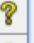

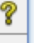

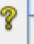

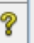

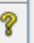
Break 100  
Hydro Connections

General		Show Disabled
Component Name	unnamed	
Component Number	100	
Break Type	[0] No Tables	
Temperature Table Option	[0] Enter liquid/gas temp	
Fluid State Option	[0] Last Interp State Held Const.	
Description	<none>	
Inlet	Pipe 80 Cell 5 outlet	
Length	0.03 (m)	
Volume	1.520122E-5 (m³)	
Initial Gas Volume Fraction	0.0 (-)	
Initial Mixture Temperature	300.0 (K)	
Initial Pressure	1.01352E5 (Pa)	
Initial Noncondensable PP	0.0 (Pa)	
Adjacent Pressure Flag	<input type="radio"/> True <input checked="" type="radio"/> False	
Max Pressure Change Rate	1.0E20 (Pa/s)	

Valve 71  
 Hydro Connections

Friction	Kfac ( 0.0, 0.0, 0.0 )	E		
Fluid Power Options	Not Modeled	E		
Wall Roughness	0.0 (m)			
Inlet	Tee 60 Cell 1 inlet	E		
Outlet	Break 90 Cell 1 inlet	E		
Valve Interface Index	Edge 2 of 3			
Flow Area Adjustment Type	[0] Flow Area Fraction per Second			
Internal Loss Model	[0] On			
Maximum Valve Rate	100.0 (1/s)			
Off Adjustment Rate	100.0 (1/s)			
Minimum Position	0.0 (-)			
Maximum Position	1.0 (-)			
Valve Flow Area	5.07E-4 (m²)			
Valve Hydro Diameter	0.0254 (m)			
Initial Flow Area Fraction	0.0 (-)			
Valve Stem Position	0.0 (-)			
Check Valve Type	[0] Static Pressure/Flow with Hysteresis			
Open Delta Pressure	1000.0 (Pa)			
Leak Area Ratio	0.0 (-)			
Latch Option	[0] Open or Close Repeatedly			



**Valve 70**  

 Hydro Connections

Friction	Krac ( 0.0, 0.0, 0.0 )		
Fluid Power Options	Not Modeled		
Wall Roughness	0.0 (m)		
Inlet	Pipe 80 Cell 1 inlet		
Outlet	Tee 60 Cell 9 outlet		
Valve Interface Index	Edge <input type="text" value="2"/> of 2		
Flow Area Adjustment Type	[0] Flow Area Fraction per Second		
Internal Loss Model	[0] On		
Maximum Valve Rate	100.0 (1/s)		
Off Adjustment Rate	100.0 (1/s)		
Minimum Position	0.0 (-)		
Maximum Position	1.0 (-)		
Valve Flow Area	5.07E-4 (m <sup>2</sup> )		
Valve Hydro Diameter	0.0254 (m)		
Initial Flow Area Fraction	0.0 (-)		
Valve Stem Position	0.0 (-)		
Check Valve Type	[0] Static Pressure/Flow with Hysteresis		
Open Delta Pressure	1000.0 (Pa)		
Leak Area Ratio	0.0 (-)		
Latch Option	[0] Open or Close Repeatedly		

## BIBLIOGRAPHY

### References

- [1] West, C. D., *Liquid Piston Stirling Engines*, Van Nostrand Reinhold, New York, 1983.
- [2] West, C. D., "Dynamic Analysis of the Fluidyne," Paper No. 839126, Proceedings of the 18th IECEC, 1983.
- [3] West, C. D., "Stirling Engines and Irrigation Pumping," Oak Ridge National Laboratory, August 1987.
- [4] West, C.D., "Liquid-Piston Stirling Machines," 2<sup>nd</sup> International Conference on Stirling Engines, Chinese Society of Naval Architecture and Marine Engineering and Chinese Society of Engineering Thermophysics, Shanghai, China, June 21-24, 1984.
- [5] West, C.D., and Fauvel, O.R., "Excitation of Displacer Motion in a Fluidyne Analysis and Experiment," Oak Ridge National Laboratory.
- [6] Walker, G., Fauvel, O.R., and Reader, G.T., "Excitation of Fluidyne Tuning Line," University of Calgary, Calgary, Alberta, Canada.
- [7] Van de Ven, J. D., and Li, P. Y., "Liquid Piston Gas Compression," *Applied Energy*, 2008.
- [8] Van de Ven, J. D., "Mobile hydraulic power supply: Liquid piston Stirling engine pump", *Renewable Energy*, Volume 34, Issue 11, November 2009, pp. 2317-2322.
- [9] Van de Ven, J. D., Gaffuri, P. B., Mies, B. J., Cole, G., "Developments Towards a Liquid Piston Stirling Engine," International Energy Conversion Engineering Conference, AIAA, Cleveland, OH, 2008.
- [10] Elston, M.J., Lurie, M.S., Rallis, C.J., and Kilgour, D.B., "Design and Development of a Liquid Piston Stirling Engine," 17<sup>th</sup> Intersociety Energy Conversion Engineering Conference, IECED, Los Angeles, California, August 8-12 1982.
- [11] Kyei-Manu, F., and Obodoako, A., "Futher Development of the Fluidyne Liquid-Piston Engine," Swarthmore College, Swarthmore, PA, May 2, 2006.
- [12] Goldberg, L. F., "A Computer Simulation and Experimentil Development of Liquid Piston Stirling Cycle Engines," MSc Thesis, Dept. of Mechanical Engineering, University of the Witwatersrand (1979).
- [13] Ozdemir, M., and Ozguc, A. F., "A Simple Mathematical Model to Analyze a Fluidyne Heat Machine", *Proceedings of the Institution of Mechanical Engineers, Part A: Journal of Power and Energy*, Volume 217, no. 1, February 1, 2003, pp. 91-100.

## Academic Vita

### School Address

346 E. Prospect Ave  
State College, PA 16801  
443-883-0970

**Andrew T. Kriebel**  
atkriebel@gmail.com

### Permanent Address

745 Buckeye Ct  
Millersville, MD 21108  
410-987-9896

### Education

#### **The Pennsylvania State University**

##### ***Schreyer Honors College***

B.S. Mechanical Engineering  
Engineering Leadership Development Minor  
Thesis: Computer Modeling Liquid Piston Stirling Engines

Graduation: May 2014

#### **University of New South Wales** (Sydney, Australia)

Foreign Exchange

February – June 2012

#### **TAFE Institute of New South Wales** (Sydney, Australia)

Vocational Training in Machining and Measurement

### Work Experience

#### **Vibration Monitoring, Research and Development Intern**

##### **KCF Technologies** (State College, PA)

January 2014 – Present

- Diagnose mechanical problems in machinery through vibration monitoring
- Research and development of new technologies for vibration sensors

#### **Mechanical Engineering Intern**

##### **GE Aviation** (Cincinnati, OH)

June - August 2013

- Conducted fuel efficiency improvement testing for US Navy gas turbine engines
- Collaborated on new product development for marine mechanical drive engine system

#### **Mechanical Engineering Intern**

##### **Johns Hopkins Applied Physics Lab** (Laurel, MD)

May 2011 – August 2012

- Evaluated feasibility, modeled, and designed mobile ground surveillance systems
- Designed electronics packaging and electronics assemblies (CAD)

#### **Engineering Communication Teaching Intern**

##### **Penn State Dept. of Eng. (UTree)** (University Park, PA)

August 2011 – Present

- Study methods of effective communication of technical topics
- Instruct Penn State and international students about effective audio/visual presentations

#### **Backpacking Trip Leader / Orientation Leader**

##### **ORION Freshman Wilderness Experience** (University Park, PA)

July – August 2011

- Led six day wilderness experience backpacking trip for crews of eight freshman students

### Leadership & Activities

#### **Tau Kappa Epsilon Fraternity**

##### **Vice President**

January – December 2013

- Oversee chapter officers/positions, recruitment, and community service

##### **Philanthropy and Dance Marathon Chair**

February 2013 – Present

- Execute fundraising of \$150,000+ for pediatric cancer research

##### **Penn State Dance Marathon, Dancer, Morale & Special Events Committees**

Fall 2010-Spring 2013

##### **Boy Scouts of America Troop 993, Eagle Scout**

Earned August 2009

- Planned & built bio-retention gardens for Eagle project

### Awards & Honors

Fulbright Scholar Finalist (Alternate), Evan Pugh Senior Award; Evan Pugh Junior Award; Boeing Outstanding Junior Award; Tau Beta Pi Engineering Honors Society; President's Sparks Award; President's Freshman Award; Phi Kappa Phi Honors Society; Phi Eta Sigma Honors Society; Tau Kappa Epsilon Scholarship Award